

this document downloaded from

vulcanhammer.info

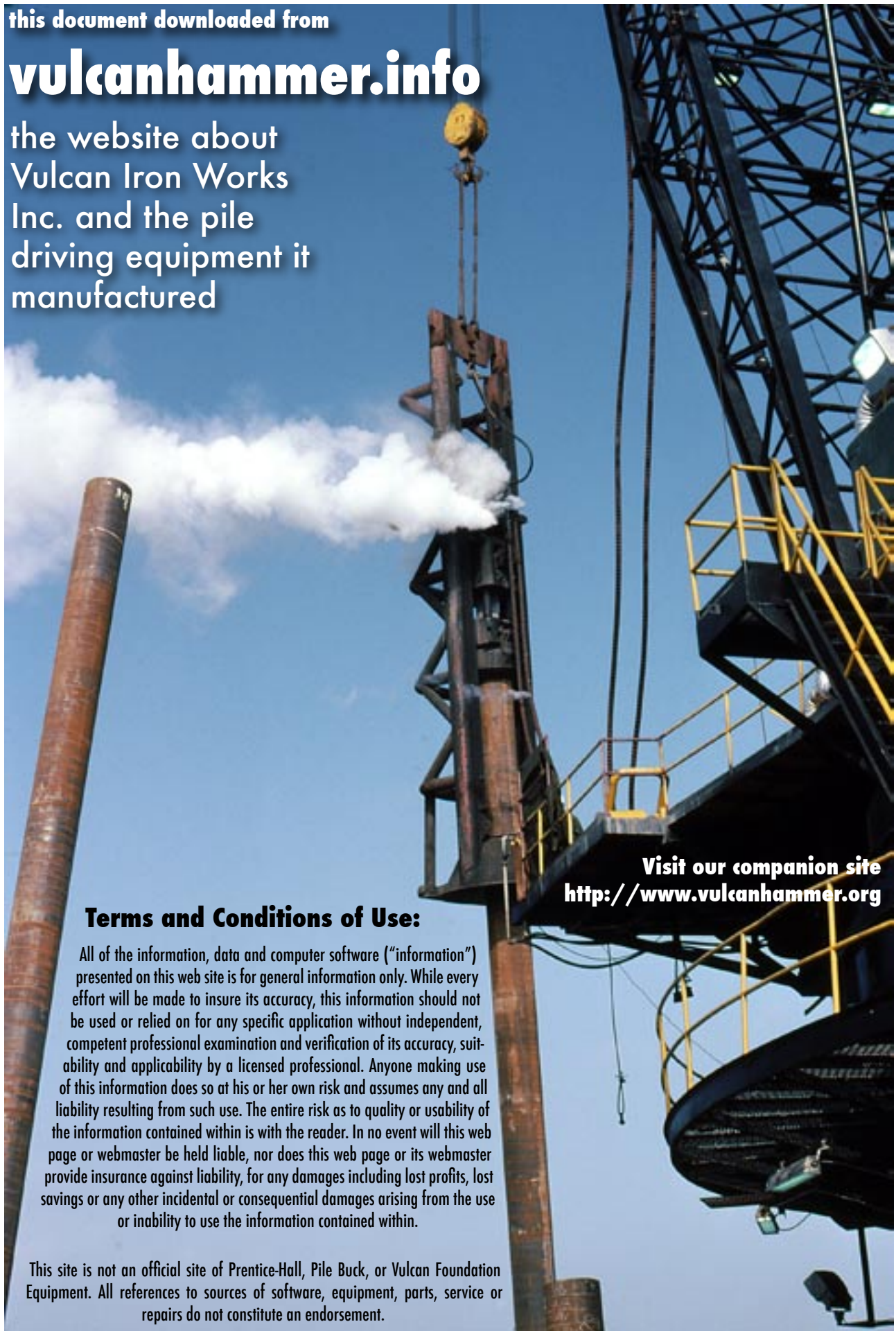
the website about
Vulcan Iron Works
Inc. and the pile
driving equipment it
manufactured

Terms and Conditions of Use:

All of the information, data and computer software ("information") presented on this web site is for general information only. While every effort will be made to insure its accuracy, this information should not be used or relied on for any specific application without independent, competent professional examination and verification of its accuracy, suitability and applicability by a licensed professional. Anyone making use of this information does so at his or her own risk and assumes any and all liability resulting from such use. The entire risk as to quality or usability of the information contained within is with the reader. In no event will this web page or webmaster be held liable, nor does this web page or its webmaster provide insurance against liability, for any damages including lost profits, lost savings or any other incidental or consequential damages arising from the use or inability to use the information contained within.

This site is not an official site of Prentice-Hall, Pile Buck, or Vulcan Foundation Equipment. All references to sources of software, equipment, parts, service or repairs do not constitute an endorsement.

Visit our companion site
<http://www.vulcanhammer.org>



Dynamic Stiffness and Damping of Piles

MILOS NOVAK

Faculty of Engineering Science, University of Western Ontario, London, Ontario N6A 3K7

Received, February 6, 1974

Accepted June 4, 1974

Dynamic response of footings and structures supported by piles can be predicted if dynamic stiffness and damping generated by soil-pile interaction can be defined. An approximate analytical approach based on linear elasticity is presented, which makes it possible to establish the dimensionless parameters of the problem and to obtain closed-form formulas for pile stiffness and damping. All components of the motion in a vertical plane are considered; that is, horizontal as well as vertical translations and rotation of the pile head. The stiffness and damping of piles are defined in such a way that the design analysis of footings and structures resting on piles can be conducted in the same way as is applied in the case of shallow foundations.

La réponse dynamique de semelles et de structures supportées par des pieux peut être prédite si la rigidité dynamique et l'amortissement produits par l'interaction sol-pieu peut être définie. Une méthode analytique approchée, basée sur l'hypothèse d'élasticité linéaire, est présentée, qui permet d'établir les paramètres adimensionnels du problème et d'obtenir des formules condensées pour la rigidité et l'amortissement du pieu. Toutes les composantes du déplacement dans un plan vertical sont considérées, c'est-à-dire les translations verticale et horizontale et la rotation de la tête du pieu. La rigidité et l'amortissement des pieux sont définies de telle façon que l'analyse de semelles et de structures fondées sur pieux puisse être conduite de la même manière que pour les fondations superficielles.

[Traduit par la Revue]

Introduction

Dynamics of piles has been receiving attention mainly due to its applications in machinery foundations and structures exposed to dynamic loads such as wind or earthquake. However, the dynamic behavior of piles is far from completely understood as the soil-pile interaction is very complex. There are no readily applicable methods available that would include this interaction and as a result of this, it is not uncommon to ignore the soil entirely and to attribute all the foundation stiffness to the stiffness of the piles. On the other hand, some approaches are used in which the horizontal and rotational stiffness of piles are ignored and all the dynamic stiffness is attributed to the soil. Damping derived from piles is in practice only guessed.

More rigorous approaches were applied by Tajimi 1966, who used a linear elastic medium model, and by Penzien 1970 who assumed a lumped mass model which made it possible to incorporate soil nonlinearity. These sophisticated solutions deal with earthquake excitation and their complexity makes them accessible to researchers rather than to practicing engineers.

The objective of this paper is to examine an

alternative approach which would approximately account for soil-pile interaction in a relatively simple manner. Such an approach can be based on the same assumption as that quite successfully applied to embedded footings (Baranov 1967; Novak and Beredugo 1972; Novak and Sachs 1973; Novak 1974); it is assumed that the soil is composed of a set of independent infinitesimally thin horizontal layers that extend to infinity.¹ This model can be viewed as a generalized Winkler's medium which possesses inertia and the capability to dissipate energy. It is further assumed that the piles are vertical, do not affect each other, and that the motion of the pile is harmonic and limited to a vertical plane. Then, both the dynamic soil reactions per unit length of the pile and the solution of the pile response can be described by closed form formulas.

Though the derivation of the approach requires a certain amount of theoretical analysis, the practical application of it can be very simple. The reader interested in design analysis need only refer to the chapter on response of pile foundations.

¹For some mathematical features of this model see Novak and Sachs 1973.

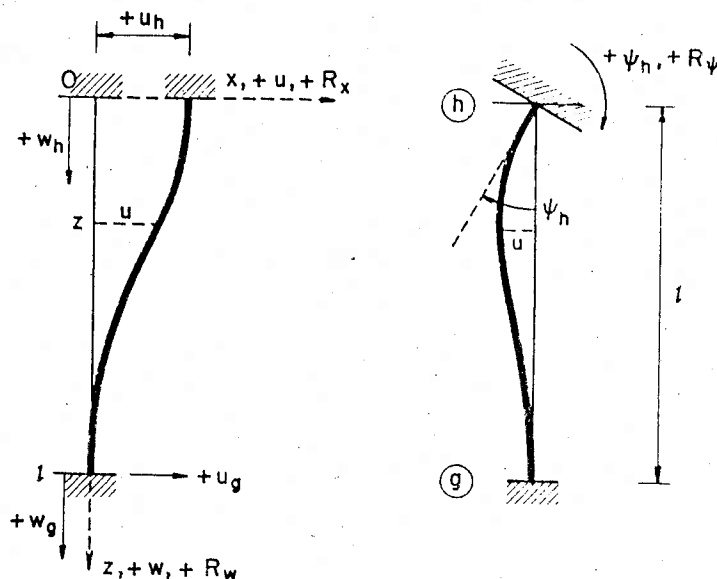


FIG. 1. Displacements and reactions of piles.

Horizontal Translation and Rotation in the Vertical Plane

Consider first the cases in which the pile is excited by horizontal translation of its head and by rotation of its head in the vertical plane (Fig. 1). Only lateral displacement of pile elements is considered. The effect of the static axial force is not accounted for in the first part of the paper but is considered separately later.

When a pile element dz undergoes a complex horizontal displacement $u(z, t)$ at height z , it will meet a horizontal soil reaction which with the above assumptions is equal to

$$[1] \quad G(S_{u1} + iS_{u2})u(z, t)dz$$

in which G = shear modulus of soil and $i = \sqrt{-1}$. Parameters S_{u1} and S_{u2} are functions of dimensionless frequency $a_0 = r_0\omega\sqrt{\rho/G}$, depend on Poisson's ratio ν , and are the real and imaginary parts of the complex function

$$[2] \quad S_u(a_0, \nu) = G[S_{u1}(a_0, \nu) + iS_{u2}(a_0, \nu)] \\ = 2\pi Ga_0$$

$$\times \frac{\frac{1}{\sqrt{q}} H_2^{(2)}(a_0) H_1^{(2)}(x_0) + H_1^{(2)}(x_0) H_1^{(2)}(a_0)}{H_0^{(2)}(a_0) H_2^{(2)}(x_0) + H_0^{(2)}(x_0) H_2^{(2)}(a_0)}$$

where r_0 = pile radius, ω = frequency, and ρ = mass density of soil.

In Eq. [2], $q = (1 - 2\nu)/2(1 - \nu)$, $x_0 = a_0\sqrt{2}$ and $H_n^{(2)}$ = Hankel functions of the second kind of order n . Equation [2] was derived by Baranov 1967. Parameters S_{u1} and S_{u2} were calculated for several values of Poisson's ratio in Beredugo and Novak 1972, in which polynomial approximations to them are also given. The parameters S are shown in Fig. 2.

With soil reaction given by Eq. [1], the differential equation of the pile horizontal damped vibration is

$$[3] \quad \mu \frac{\partial^2 u(z, t)}{\partial t^2} + c \frac{\partial u(z, t)}{\partial t} + G(S_{u1} + iS_{u2}) \\ \times u(z, t) + E_p I \frac{\partial^4 u(z, t)}{\partial z^4} = 0$$

in which μ = mass of the pile per unit length, c = coefficient of pile internal damping, and $E_p I$ = bending stiffness of the pile.

Assume a harmonic motion induced through the pile ends.

Then a steady-state (particular) solution to Eq. [3] can be written as

$$[4] \quad u(z, t) = u(z)e^{i\omega t}$$

where complex amplitude

$$[5] \quad u(z) = u_1(z) + iu_2(z)$$

Substitution of Eq. [4] into Eq. [3] yields an ordinary differential equation:

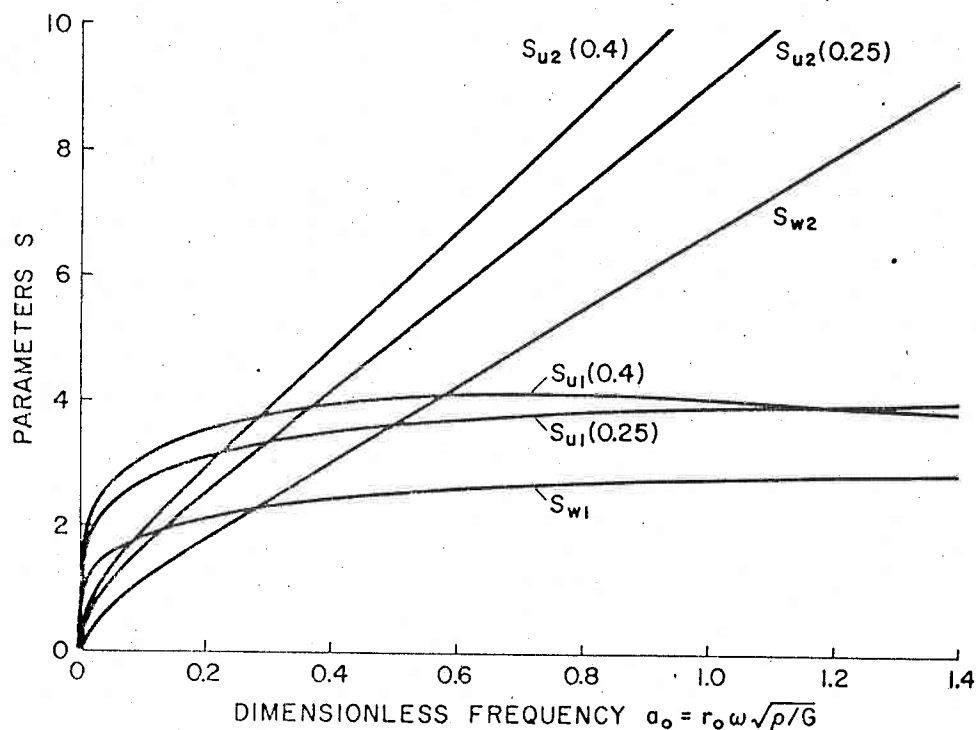


FIG. 2. Parameters S_{u1} , S_{u2} , S_{w1} , and S_{w2} , (Poisson's ratio given in brackets).

$$[6] \quad E_p I \frac{d^4 u(z)}{dz^4} + u(z)$$

$$\times [GS_{u1} - \mu\omega^2 + i(c\omega + GS_{u2})] = 0$$

The general solution to this equation is

$$[7] \quad u(z) = C_1 \cosh \lambda \frac{z}{l} + C_2 \sinh \lambda \frac{z}{l} \\ + C_3 \cos \lambda \frac{z}{l} + C_4 \sin \lambda \frac{z}{l}$$

in which complex frequency parameter

$$[8] \quad \lambda =$$

$$l \sqrt{\frac{1}{E_p I} [\mu\omega^2 - GS_{u1} - i(c\omega + GS_{u2})]}$$

Note

$$[9] \quad \lambda_0 = l \sqrt[4]{\frac{\mu\omega^2}{E_p I}}, \quad L = \frac{l^4 G}{E_p I}$$

$$a = \lambda_0^4 - LS_{u1},$$

$$[10] \quad b = -L(c\omega \frac{1}{G} + S_{u2})$$

and

$$[11] \quad r = \sqrt{a^2 + b^2}, \quad \tan \phi = \frac{b}{a}$$

Then, parameter λ is more conveniently described as

$$[12] \quad \lambda = \lambda_1 + i\lambda_2$$

in which real and imaginary parts of λ are

$$[13] \quad \lambda_1 = \sqrt[4]{r} \cos \frac{\phi}{4}, \quad \lambda_2 = \sqrt[4]{r} \sin \frac{\phi}{4}$$

For a pile of circular cross section the parameters given by Eq. [9] are also

$$[14] \quad L = \frac{4}{\pi} \frac{G}{E_p} \left(\frac{l}{r_0} \right)^4 = \frac{4}{\pi} \frac{\rho}{\rho_p} \left(\frac{V_s}{v_c} \right)^2 \left(\frac{l}{r_0} \right)^4$$

and

$$[15] \quad \lambda_0 = \frac{l}{r_0} \sqrt[4]{\frac{4}{\rho} \frac{\rho_p G}{E_p}} \sqrt{a_0} = \frac{l}{r_0} \sqrt[4]{\frac{2}{v_c} \frac{V_s}{v_c}} \sqrt{a_0}$$

in which $V_s = \sqrt{G/\rho}$ = shear wave velocity of soil and $v_c = \sqrt{E_p/\rho_p}$ = longitudinal wave velocity in the pile. The dimensionless parameters

The problem obviously are slenderness ratio l/r_0 , mass ratio ρ/ρ_p , and wave velocity ratio V_s/r_c .

Integration constants C are given by boundary conditions for whose application the displacement derivatives are also needed:

$$[16] \left\{ \begin{aligned} \frac{du(z)}{dz} &= \frac{\lambda}{l} \left(C_1 \sinh \lambda \frac{z}{l} + C_2 \cosh \lambda \frac{z}{l} \right. \\ &\quad \left. - C_3 \sin \lambda \frac{z}{l} + C_4 \cos \lambda \frac{z}{l} \right) \\ \frac{d^2u(z)}{dz^2} &= \frac{\lambda^2}{l^2} \left(C_1 \cosh \lambda \frac{z}{l} + C_2 \sinh \lambda \frac{z}{l} \right. \\ &\quad \left. - C_3 \cos \lambda \frac{z}{l} - C_4 \sin \lambda \frac{z}{l} \right) \\ \frac{d^3u(z)}{dz^3} &= \frac{\lambda^3}{l^3} \left(C_1 \sinh \lambda \frac{z}{l} + C_2 \cosh \lambda \frac{z}{l} \right. \\ &\quad \left. + C_3 \sin \lambda \frac{z}{l} - C_4 \cos \lambda \frac{z}{l} \right) \end{aligned} \right.$$

With these derivatives the bending moments are as usual

$$M = -E_p I \frac{d^2u(z)}{dz^2}$$

and the shear forces

$$[18] \quad T = -E_p I \frac{d^3u(z)}{dz^3}$$

The dynamic stiffness of the pile can be determined as the end force producing a unit displacement of the pile head (or tip). This unit displacement and the other end conditions represent the boundary conditions from which the integration constants C can be established.

Equations [7] and [16] do not formally differ from those of ordinary prismatic bars and therefore, the integration constants that are actually functions of λ , are the same as with such bars. The effects of soil enter the problem only through the parameter λ .

To solve the response of footings and structures supported by piles it is necessary to know the relation between the pile reactions at the level of the pile head and the motions of the pile upper and lower ends² (Fig. 1). With the integration constants being formally the same as in absence of the soil, the end reactions are

readily obtained from Eqs. [17] and [18]. Using the notation after Kolousek 1973, the horizontal pile head reaction R_x and the end moment reaction R_ψ are for both ends fixed:³

$$[19] \quad R_x(t) = -\frac{E_p I}{l^3} F_6(\lambda) u_h(t) - \frac{E_p I}{l^2} F_4(\lambda) \psi_h(t) - \frac{E_p I}{l^3} F_5(\lambda) u_g(t)$$

$$[20] \quad R_\psi(t) = -\frac{E_p I}{l^2} F_4(\lambda) u_h(t) - \frac{E_p I}{l} F_2(\lambda) \psi_h(t) - \frac{E_p I}{l^2} F_3(\lambda) u_g(t)$$

Here, u_h , ψ_h = the pile head translation and rotation, respectively, u_g = horizontal translation of the pile lower end and functions

$$[21] \left\{ \begin{aligned} F_2(\lambda) &= -\lambda \frac{\cosh \lambda \sin \lambda - \sinh \lambda \cos \lambda}{\cosh \lambda \cos \lambda - 1} = F_2(\lambda)_1 + iF_2(\lambda)_2 \\ F_3(\lambda) &= -\lambda^2 \frac{\cosh \lambda - \cos \lambda}{\cosh \lambda \cos \lambda - 1} = F_3(\lambda)_1 + iF_3(\lambda)_2 \\ F_4(\lambda) &= \lambda^2 \frac{\sinh \lambda \sin \lambda}{\cosh \lambda \cos \lambda - 1} = F_4(\lambda)_1 + iF_4(\lambda)_2 \\ F_5(\lambda) &= \lambda^3 \frac{\sinh \lambda + \sin \lambda}{\cosh \lambda \cos \lambda - 1} = F_5(\lambda)_1 + iF_5(\lambda)_2 \\ F_6(\lambda) &= -\lambda^3 \frac{\cosh \lambda \sin \lambda + \sinh \lambda \cos \lambda}{\cosh \lambda \cos \lambda - 1} = F_6(\lambda)_1 + iF_6(\lambda)_2 \end{aligned} \right.$$

Subscripts 1 and 2 indicate the real and imaginary parts of functions F .

With the lower end pinned:

$$[22] \quad R_x(t) = -\frac{E_p I}{l^3} F_{11}(\lambda) u_h(t) - \frac{E_p I}{l^2} F_9(\lambda) \psi_h(t) - \frac{E_p I}{l^3} F_{10}(\lambda) u_g(t)$$

³The pile is rigidly connected to the footing (i.e. moments are transmitted) but translations and rotations of the ends are possible.

²The motion of the pile lower end would come into play when considering earthquake excitation.

$$[23] \quad R_\psi(t) = -\frac{E_p I}{l^2} F_9(\lambda) u_h(t) \\ - \frac{E_p I}{l} F_7(\lambda) \psi_h(t) - \frac{E_p I}{l^2} F_8(\lambda) u_g(t)$$

in which

$$[24] \quad \left\{ \begin{array}{l} F_7(\lambda) = \lambda \frac{2 \sinh \lambda \sin \lambda}{\cosh \lambda \sin \lambda - \sinh \lambda \cos \lambda} = F_7(\lambda)_1 + iF_7(\lambda)_2 \\ F_8(\lambda) = \lambda^2 \frac{\sinh \lambda + \sin \lambda}{\cosh \lambda \sin \lambda - \sinh \lambda \cos \lambda} = F_8(\lambda)_1 + iF_8(\lambda)_2 \\ F_9(\lambda) = -\lambda^2 \frac{\cosh \lambda \sin \lambda + \sinh \lambda \cos \lambda}{\cosh \lambda \sin \lambda - \sinh \lambda \cos \lambda} = F_9(\lambda)_1 + iF_9(\lambda)_2 \\ F_{10}(\lambda) = -\lambda^3 \frac{\cosh \lambda + \cos \lambda}{\cosh \lambda \sin \lambda - \sinh \lambda \cos \lambda} = F_{10}(\lambda)_1 + iF_{10}(\lambda)_2 \\ F_{11}(\lambda) = \lambda^3 \frac{2 \cosh \lambda \cos \lambda}{\cosh \lambda \sin \lambda - \sinh \lambda \cos \lambda} = F_{11}(\lambda)_1 + iF_{11}(\lambda)_2 \end{array} \right.$$

In the above equations, reactions R , functions $F_j(\lambda)$ and displacements u and ψ are complex; functions $F_j(\lambda)_{1,2}$ are real.

For a set of typical dimensionless parameters, functions F relating to pile head motions are shown in Fig. 3. The notation is abbreviated as indicated. Subscript 1 denotes the part of F relating to dynamic stiffness; subscript 2 denotes the part relating to damping. The damping is caused by energy radiation from the pile into the soil. Internal damping of the pile was neglected ($c = 0$) in all numerical data given in this paper because it is much smaller than that of soil. The damping parts of F are shown in a reduced form as F_2/a_0 for reasons made apparent later herein.

With a particular pile, functions F strongly depend on the wave velocity ratio V_s/c_c (stiffness

of soil). This can be seen from Fig. 4 in which functions $F_{11}(\lambda)_1$ and $F_{11}(\lambda)_2/a_0$ are shown for a few values of the wave velocity ratio, all other parameters remaining the same as in Fig. 3.

The approach presented is approximate in its basic assumption and therefore a comparison with a more 'rigorous' approach is important. Such a comparison is made in Fig. 5 where the approximate solution for the most important function F_{11} is shown together with the results obtained by T. Nogami and the author using a more rigorous theory. The latter theory assumes a homogeneous stratum overlying a rigid bedrock and the results are obtained by means of modal analysis. In this approach the theory, used first by Tajimi 1966, was modified and extended. (The more rigorous solution is not quite exact because the boundary conditions on the soil surface are not completely satisfied and the convergence of the results is slow.)

The differences between the two solutions appear acceptable and diminish with increasing frequency. The approximate solution does not yield the peaks caused by soil layer resonances. The sharpness of the peaks strongly depends on soil viscosity and the peaks can actually vanish with higher viscosity. There are no experiments known to the author which would prove the existence of such peaks in pile stiffness and damping parameters. The rigorous solution yields slightly larger stiffness and hence, the approximate solution is on the safe side because there is no perfect bond between the pile and the soil as the theory assumes.

Functions F could be used as they are defined. However, it will be seen later that the results can be presented in a modified form that eliminates the need for their calculation in most practical applications.

Vertical Vibrations

The dynamic reactions of the pile pertinent to vertical motion of the pile head can be obtained using the same assumptions for soil as in the previous case. Assume further that the lower end of the pile is fixed.

Then, the vertical soil reaction acting at height z on pile element dz is (Baranov 1967; Novak and Beredugo 1972):

$$[25] \quad G(S_{w1} + iS_{w2})w(z, t)dz$$

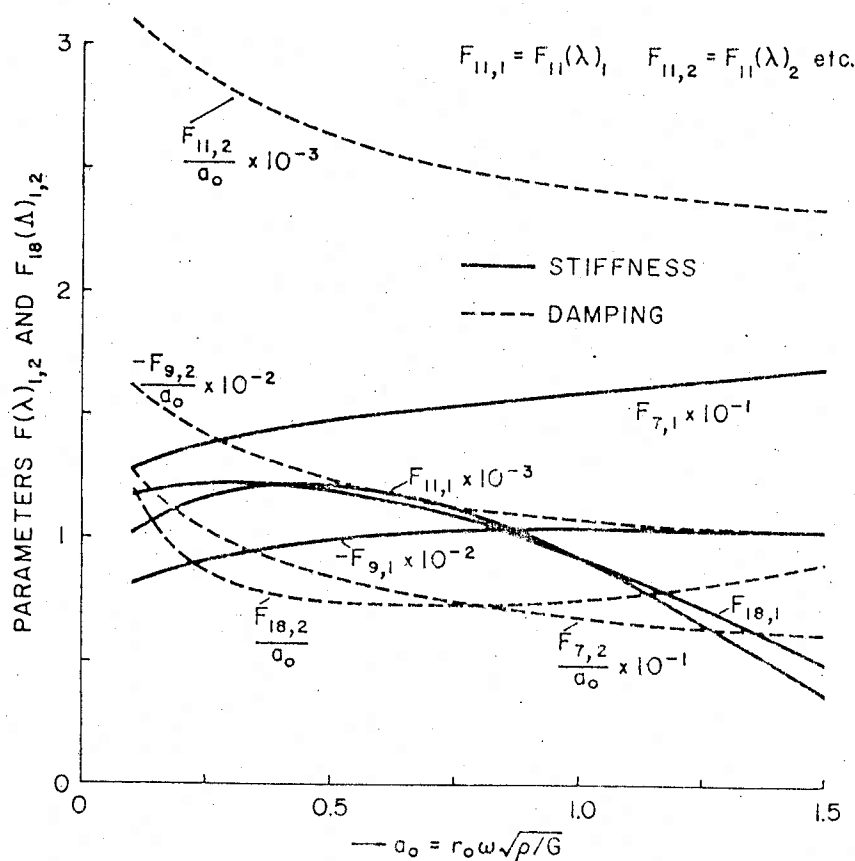


FIG. 3. Functions F for dynamic stiffness and geometric damping of piles for a typical set of dimensionless parameters, ($l/r_0 = 40$, $V_s/v_c = 0.003$, $\rho/\rho_r = 0.7$, $\nu = 0.4$).

in which

$$[26] \quad S_{w1} = 2\pi a_0 \frac{J_1(a_0)J_0(a_0) + Y_1(a_0)Y_0(a_0)}{J_0^2(a_0) + Y_0^2(a_0)}$$

$$[27] \quad S_{w2} = \frac{4}{J_0^2(a_0) + Y_0^2(a_0)}$$

Herein $J_0(a_0)$, $J_1(a_0)$ = Bessel functions of the first kind of order zero and one, respectively, and $Y_0(a_0)$, $Y_1(a_0)$ = Bessel functions of the second kind of order zero and one. Functions S_{w1} and S_{w2} are shown in Fig. 2.

With the soil reactions defined by Eq. [25], the differential equation of damped axial vibration $w(z, t)$ of the pile is:

$$[28] \quad \mu \frac{\partial^2 w(z, t)}{\partial t^2} + c \frac{\partial w(z, t)}{\partial t} - E_p A \frac{\partial^2 w(z, t)}{\partial z^2} + G(S_{w1} + iS_{w2})w(z, t) = 0$$

in which A = area of the pile cross section.

With a harmonic motion (induced through boundary conditions) displacement

$$[29] \quad w(z, t) = w(z)e^{i\omega t}$$

and Eq. [28] yields an ordinary differential equation

$$[30] \quad w(z)[- \mu \omega^2 + i c \omega + G(S_{w1} + iS_{w2})] - E_p A \frac{d^2 w(z)}{dz^2} = 0$$

The solution to this equation is

$$[31] \quad w(z) = C_s \cos \Lambda \frac{z}{l} + C_c \sin \Lambda \frac{z}{l}$$

in which the complex frequency parameter is in this case

$$[32] \quad \Lambda = l \sqrt{\frac{1}{E_p A} [\mu \omega^2 - G S_{w1} - i(c\omega + G S_{w2})]}$$

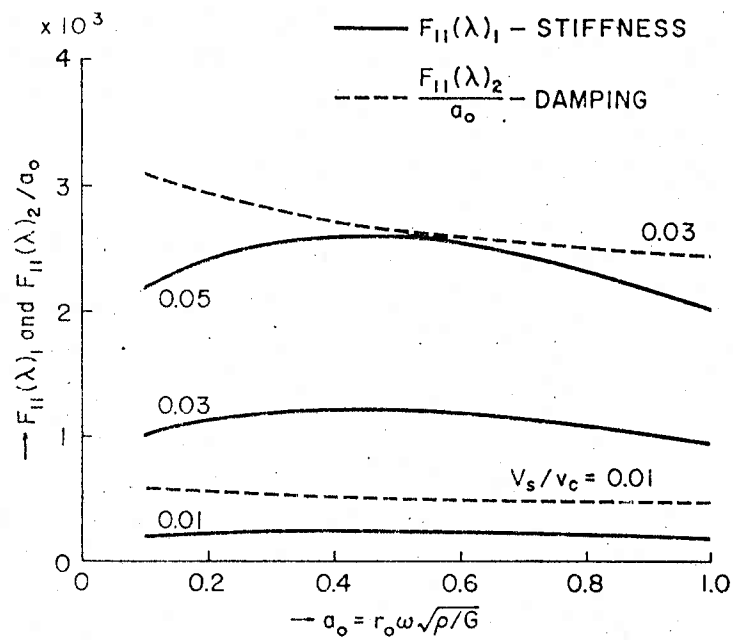


FIG. 4. Variations of function $F_{11}(\lambda)$ with frequency a_0 and wave velocity ratio V_s/v_c (stiffness of soil), ($l/r_0 = 40$, $\rho/\rho_p = 0.7$, $\nu = 0.4$).

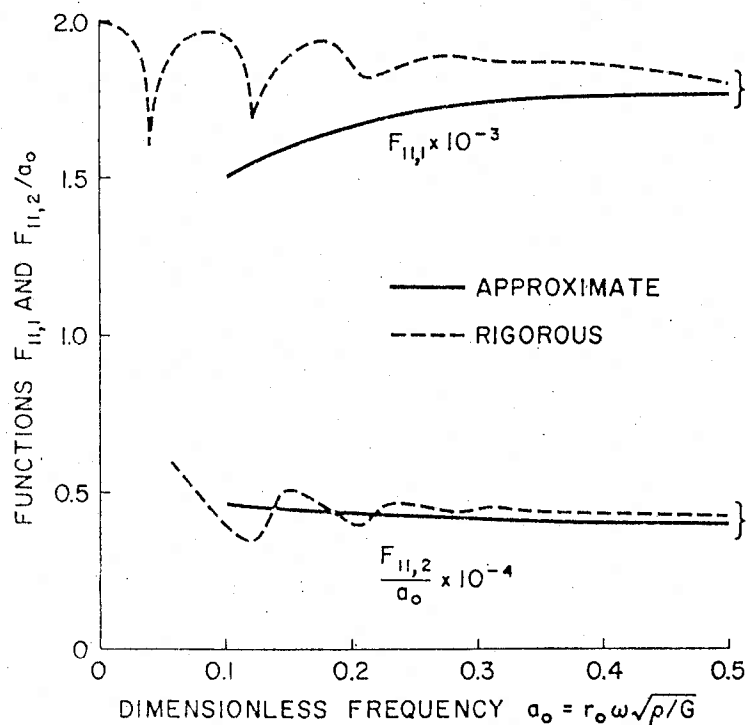


FIG. 5. Comparison of results obtained by approximate solution and by more rigorous solution, ($l/r_0 = 38.5$; $V_s/v_c = 0.044$, $\rho/\rho_p = 0.625$, $\nu = 0.4$).

$$\Lambda_0 = l \sqrt{\frac{\mu \omega^2}{E_p A}}, \quad K = \frac{l^2 G}{E_p A}$$

which is for a pile of circular cross section

$$\Lambda_0 = \frac{l}{r_0} \sqrt{\frac{\rho_p G}{\rho E_p}} a_0 = \frac{l}{r_0} \frac{V_s}{v_c} a_0$$

$$K = \frac{1}{\pi} \frac{G}{E_p} \left(\frac{l}{r_0} \right)^2 = \frac{1}{\pi} \frac{\rho}{\rho_p} \left(\frac{V_s l}{v_c r_0} \right)^2$$

Note further

$$a = \Lambda_0^2 - K S_{w1}, \quad b = -K \left(c \omega \frac{1}{G} + S_{w2} \right)$$

where r and ϕ are obtained from Eqs. [11] and parameter Λ is

$$\Lambda = \Lambda_1 + i\Lambda_2$$

which

$$\Lambda_1 = \sqrt{r} \cos \frac{\phi}{2}, \quad \Lambda_2 = \sqrt{r} \sin \frac{\phi}{2}$$

Amplitude of the axial force is

$$N(z) = E_p A \frac{dw(z)}{dz}$$

from Eq. [31]

$$\frac{dw(z)}{dz} = -C_5 \frac{\Lambda}{l} \sin \Lambda \frac{z}{l} + C_6 \frac{\Lambda}{l} \cos \Lambda \frac{z}{l}$$

Integration constants C_5 and C_6 are obtained from the end conditions. Due to complex motions of pile head $w_h(t)$ (Fig. 1) and pile lower end $w_g(t)$, the vertical reaction of pile $R_w(t)$ at the level of the pile head is

$$R_w(t) = -\frac{E_p A}{l} F_{18}(\Lambda) w_h(t) + \frac{E_p A}{l} F_{19}(\Lambda) w_g(t)$$

which

$$\begin{cases} F_{18}(\Lambda) = \Lambda \cotan \Lambda = \\ F_{18}(\Lambda)_1 + iF_{18}(\Lambda)_2 \\ F_{19}(\Lambda) = \Lambda \operatorname{cosec} \Lambda = \\ F_{19}(\Lambda)_1 + iF_{19}(\Lambda)_2 \end{cases}$$

scripts 1 and 2 denote the real and imaginary parts of the functions. An example of $F_{18}(\Lambda)_{1,2}$ is shown in Fig. 3.

Equation [41] is formally equal to that of the

beam alone, Kolousek 1973. The effects of soil again enter the problem only through parameter Λ .

The agreement with the more rigorous solution is again quite good. With increasing frequency the two solutions asymptotically approach.

Stiffness and Damping Constants of Piles

With the above reactions, the motion of the pile supported body can be predicted.

If, for example, only the horizontal motion is possible, the differential equation of motion is, with respect to Eq. [22]

$$[43] \quad m \frac{d^2 u(t)}{dt^2} + \sum \frac{E_p I}{l^3} \times [F_{11}(\Lambda)_1 + iF_{11}(\Lambda)_2] u(t) = Q \exp(i\omega t)$$

where the summation extends over all the piles, m = mass of the body, $u(t)$ = the horizontal displacement of the body, and $Q \exp(i\omega t)$ = horizontal excitation.

If the body vibrates in the vertical direction under the effect of a vertical force $P \exp(i\omega t)$ the equation of motion $w(t)$ is, with the pile reaction given by Eq. [41]

$$[44] \quad m \frac{d^2 w(t)}{dt^2} + \sum \frac{E_p A}{l} \times [F_{18}(\Lambda)_1 + iF_{18}(\Lambda)_2] w(t) = P \exp(i\omega t)$$

Similar equations can be written for coupled motions.

The solution of the response from the equations of motion follows standard procedures. To facilitate the procedure and to make it actually identical to that applied with any other type of foundation, it is advantageous to define the equivalent pile stiffnesses and damping. These can be established by comparing Eqs. [43] and [44] etc. with the corresponding standard equations of footings.

The equivalent stiffness constant k^1 and damping constant c^1 of one pile are for:

Vertical translation

$$[45] \quad k_{zz}^1 = \frac{E_p A}{r_0} f_{18,1}$$

where

$$[46] \quad f_{18,1} = \frac{F_{18}(\Lambda)_1}{l/r_0}$$

$$[47] \quad c_{zz}^1 = \frac{E_p A}{V_s} f_{18,2}$$

where

$$[48] \quad f_{18,2} = \frac{F_{18}(\lambda)_2}{a_0 l / r_0}$$

Horizontal translation and the lower end pinned

$$[49] \quad k_{xx}^1 = \frac{E_p I}{r_0^3} f_{11,1}$$

where

$$[50] \quad f_{11,1} = \frac{F_{11}(\lambda)_1}{(l/r_0)^3}$$

$$[51] \quad c_{xx}^1 = \frac{E_p I}{r_0^2 V_s} f_{11,2}$$

where

$$[52] \quad f_{11,2} = \frac{F_{11}(\lambda)_2}{a_0 (l/r_0)^3}$$

Rotation of the pile head in the vertical plane

$$[53] \quad k_{\psi\psi}^1 = \frac{E_p I}{r_0} f_{7,1}$$

where

$$[54] \quad f_{7,1} = \frac{F_7(\lambda)_1}{l/r_0}$$

$$[55] \quad c_{\psi\psi}^1 = \frac{E_p I}{V_s} f_{7,2}$$

where

$$[56] \quad f_{7,2} = \frac{F_7(\lambda)_2}{a_0 l / r_0}$$

Cross-stiffness and cross-damping coefficients

$$[57] \quad k_{x\psi}^1 = \frac{E_p I}{r_0^2} f_{9,1}$$

where

$$[58] \quad f_{9,1} = \frac{F_9(\lambda)_1}{(l/r_0)^2}$$

$$[59] \quad c_{x\psi}^1 = \frac{E_p I}{r_0 V_s} f_{9,2}$$

where

$$[60] \quad f_{9,2} = \frac{F_9(\lambda)_2}{a_0 (l/r_0)^2}$$

In this approach, $k_{x\psi}^1 = k_{\psi x}^1$ and $c_{x\psi}^1 = c_{\psi x}^1$.

With the lower end fixed, corresponding functions are substituted into the above equations, i.e. F_6 in place of F_{11} , F_2 in place of F_7 , and F_4 in place of F_9 . However, the parametric study of functions F shows that the pile stiffnesses and damping are almost the same for fixed tip

and pinned tip when the slenderness ratio l/r_0 is larger than about 25 (Fig. 6). The influence of the end condition at the tip appears less than is the case with static loads (Poulos 1973).

By means of the above formulas, the stiffness and damping constants of piles can be readily established. The calculation can be greatly simplified if advantage is taken of two favorable circumstances that are evident when using stiffness and damping parameters f instead of the original frequency functions F .

Parameters $f_{i,1}$ and $f_{i,2}$ are somewhat modified functions F and are proportional to $F_{i,1}$ and $F_{i,2}/a_0$. The advantages of parameters f are that (1) they change only modestly with frequency and (2) most of them are often independent of the slenderness ratio that is of the pile length.

The variation with frequency of parameters f can be seen from Figs. 3, 4, 5, and 7. In most real situations, the dimensionless frequency a_0 is smaller than about 0.5 and for practical purposes, it seems possible to consider the stiffness and damping parameters f as constants independent of frequency.

Variations of frequency functions F with slenderness ratio l/r_0 are very strong, but these variations are much less with parameters f as can be seen from Figs. 6 and 8.

In Fig. 7, parameters f_{11} are shown for a range of frequencies and for four values of the slenderness ratio. Figure 8 shows all the parameters pertinent to horizontal translation and rotation of the pile head versus the slenderness ratio. The values shown are accurate for $a_0 = 0.3$. It can be seen that these parameters are practically independent of pile length for all slenderness ratios larger than about 20 with wave velocity ratios equal or greater than 0.03. With very soft soils featuring a wave velocity ratio of 0.01 this limit rises to about 30. These limits are quite low and make it possible to use stiffness and damping parameters independent of pile length. Such constant parameters are given in Table 1 for a few values of wave velocity ratios V_s/v_c , two values of mass ratio ρ/ρ_p and two values of Poisson's ratio ν . The mass ratios are representative of reinforced concrete and wooden piles, respectively.

The stiffness and damping parameters for the vertical motion of the pile head depend quite strongly on pile length as can be seen from Figs. 9a and b, where parameters $f_{18,1}$ and $f_{18,2}$ are

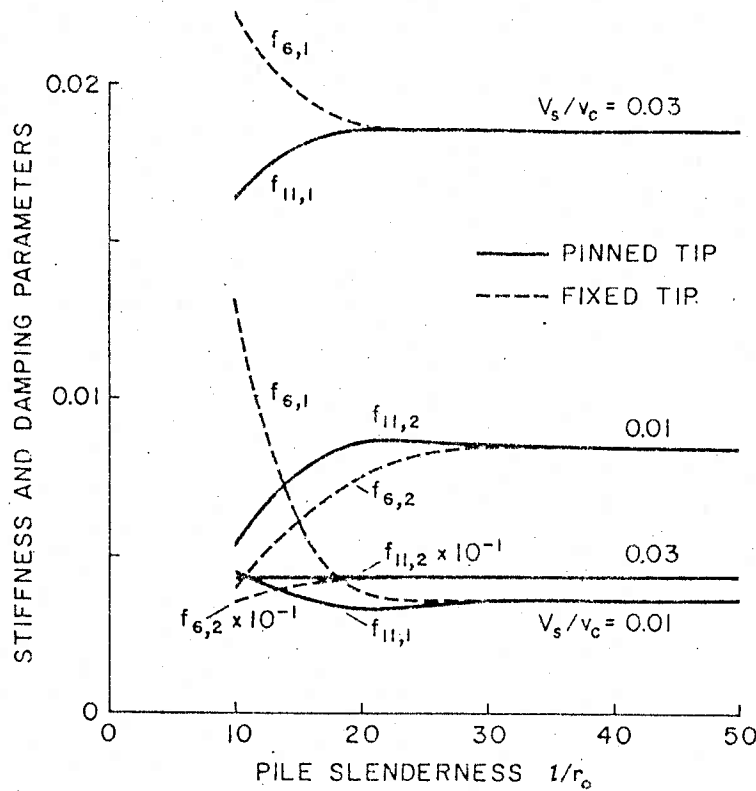


FIG. 6. Variations of stiffness and damping parameters with slenderness for pinned tip and fixed tip piles. ($\rho/\rho_p = 0.7$, $\nu = 0.4$, $a_0 = 0.3$).

given for the same input parameters as Table 1. Parameters f_{18} are independent of Poisson's ratio and can be read from Fig. 9 for a large range of slenderness and wave velocity ratios.

Table 1 and Fig. 9 make it easy to estimate the dynamic stiffness of piles and the geometric damping resulting from energy radiation.

Both stiffness and damping may be somewhat affected by pile grouping. Some considerations of this effect can be found in Barkan 1962 and Poulos 1971. No damping is, of course, obtained from a static solution (Poulos 1971).

Stiffness and Damping Constants of the Footing

The above formulas for stiffness and damping constants pertinent to the individual displacements of the pile head can be used to obtain the stiffness and damping constants including the coupled ones needed to solve the coupled response of footings and structures supported by piles.

For example, the stiffness constant for footing rocking is composed of components produced by

head rotation, vertical translation—and if the reference point lies above the pile heads, also by head horizontal translation (Fig. 10).

With rigid bodies such as footings, it is advantageous to choose the centroid for the reference point. Then the stiffness and damping constants are defined as forces that must act at the centroid to produce a sole unit displacement or unit velocity at the reference point. From this definition, the stiffness constants of the footing are

$$[61] \quad \begin{cases} k_{zz} = \sum_r k_{zz}^1 \\ k_{xx} = \sum_r k_{xx}^1 \\ k_{\psi\psi} = \sum_r (k_{\psi\psi}^1 + k_{zz}^1 x_r^2 + k_{xx}^1 z_c^2 - 2k_{x\psi}^1 z_c) \\ k_{x\psi} = k_{\psi x} = \sum_r (k_{x\psi}^1 - k_{xx}^1 z_c) \end{cases}$$

The damping constants of the footing are

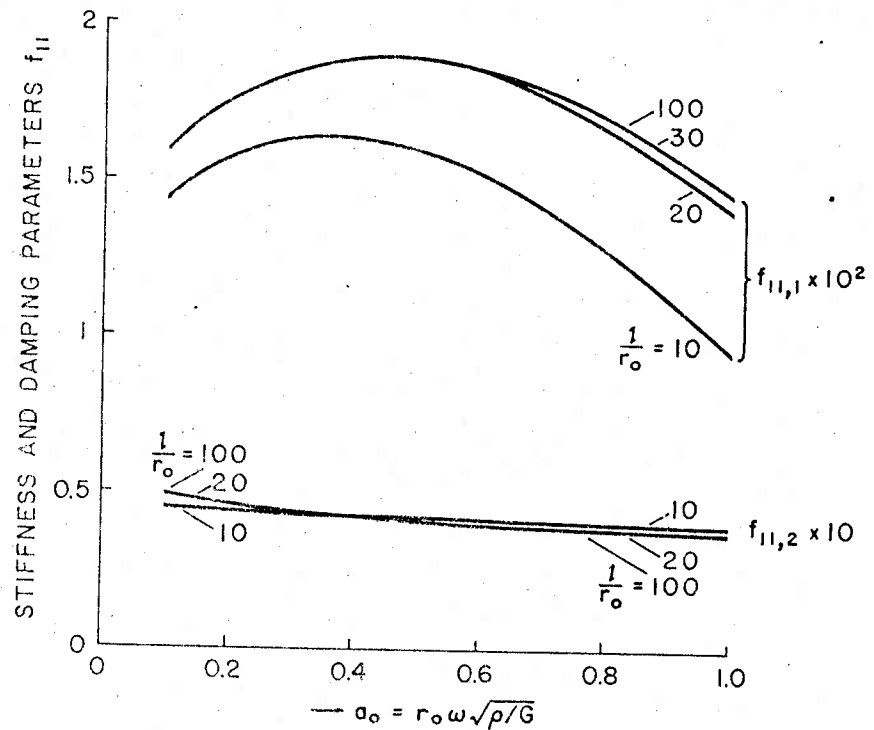


FIG. 7. Variations of stiffness and damping parameters $f_{11,1}$ and $f_{11,2}$ with frequency a_0 and slenderness ratio l/r_0 , ($V_s/v_c = 0.03$, $\rho/\rho_p = 0.7$, $\nu = 0.4$).

TABLE 1. Stiffness and damping parameters f_7, f_9, f_{11} for concrete and wooden piles with $l/r_0 > 25$

ν	$\frac{\rho}{\rho_p}$	$\frac{V_s}{v_c}$	Stiffness parameters			Damping parameters		
			$f_{7,1}$	$f_{9,1}$	$f_{11,1}$	$f_{7,2}$	$f_{9,2}$	$f_{11,2}$
0.4	0.7 (Concrete)	0.01	0.202	-0.0194	0.0036	0.139	-0.0280	0.0084
		0.02	0.285	-0.0388	0.0100	0.200	-0.0566	0.0238
		0.03	0.349	-0.0582	0.0185	0.243	-0.0848	0.0438
		0.04	0.403	-0.0776	0.0284	0.281	-0.1130	0.0674
		0.05	0.450	-0.0970	0.0397	0.314	-0.1410	0.0942
0.4	2.0 (Wood)	0.01	0.265	-0.0336	0.0082	0.176	-0.0466	0.0183
		0.02	0.374	-0.0673	0.0231	0.249	-0.0932	0.0516
		0.03	0.459	-0.1010	0.0425	0.305	-0.1400	0.0949
		0.04	0.529	-0.1350	0.0654	0.352	-0.1860	0.1460
		0.05	0.592	-0.1680	0.0914	0.394	-0.2330	0.2040
0.25	0.7 (Concrete)	0.01	0.195	-0.0181	0.0032	0.135	-0.0262	0.0076
		0.02	0.275	-0.0362	0.0090	0.192	-0.0529	0.0215
		0.03	0.337	-0.0543	0.0166	0.235	-0.0793	0.0395
		0.04	0.389	-0.0724	0.0256	0.272	-0.1057	0.0608
		0.05	0.435	-0.0905	0.0358	0.304	-0.1321	0.0850
0.25	2.0 (Wood)	0.01	0.256	-0.0315	0.0074	0.169	-0.0434	0.0165
		0.02	0.362	-0.0630	0.0209	0.240	-0.0868	0.0465
		0.03	0.444	-0.0945	0.0385	0.293	-0.1301	0.0854
		0.04	0.512	-0.1260	0.0593	0.339	-0.1735	0.1315
		0.05	0.573	-0.1575	0.0828	0.379	-0.2168	0.1838

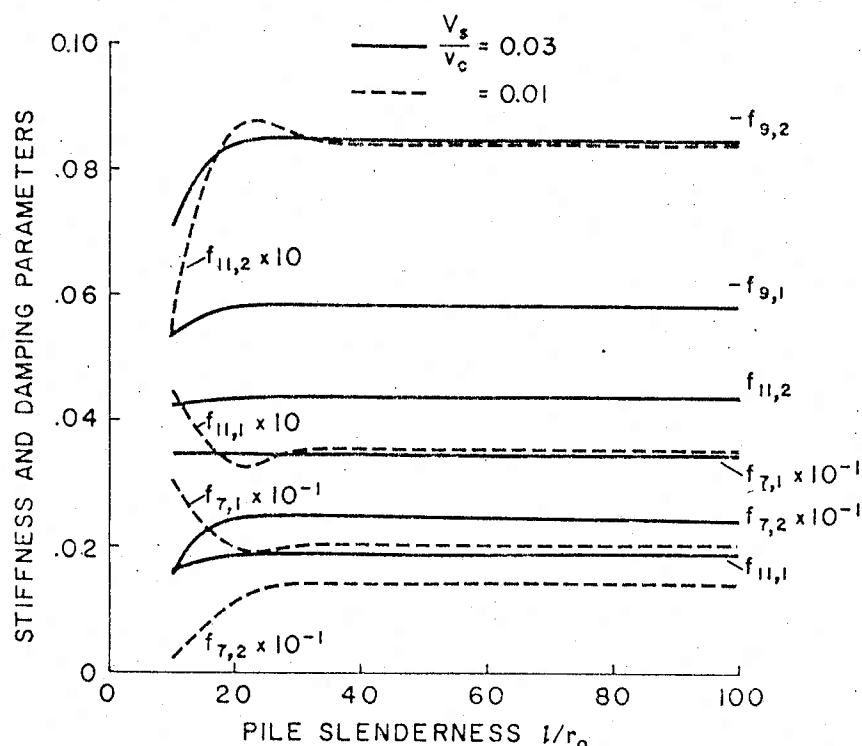


FIG. 8. Variations of stiffness and damping parameters of horizontal response with pile slenderness l/r_0 for two stiffnesses of soil, ($\rho/\rho_p = 0.7$, exact for $a_0 = 0.3$).

$$[62] \begin{cases} c_{zz} = \sum_r c_{zz}^1 \\ c_{xx} = \sum_r c_{xx}^1 \\ c_{\psi\psi} = \sum_r (c_{\psi\psi}^1 + c_{zz}^1 x_r^2 + c_{xx}^1 z_c^2 - 2c_{x\psi}^1 z_c) \\ c_{x\psi} = c_{\psi x} = \sum_r (c_{x\psi}^1 - c_{xx}^1 z_c) \end{cases}$$

can be obtained from formulae developed by Beredugo and Novak 1972 and Novak and Beredugo 1972 and summarized by Novak 1974 (Eqs. [1]–[6]). In those formulae all C and \bar{C} must be taken as zero, $G = G_s$ and $\rho = \rho_s$ to describe the properties of the backfill and equivalent radius r_0 must represent the footing not the piles. Full soil reaction in the base can, of course, be considered with equal ease if required.

The summation is taken over all the piles.

Effect of Footing Embedment

The pile-supported footing is often partially embedded as shown in Fig. 11. As a result of it, there are also soil reactions acting on the vertical sides of the footing. (The soil reactions acting on the base area need not be considered as the contact there may be lost due to soil settlement.)

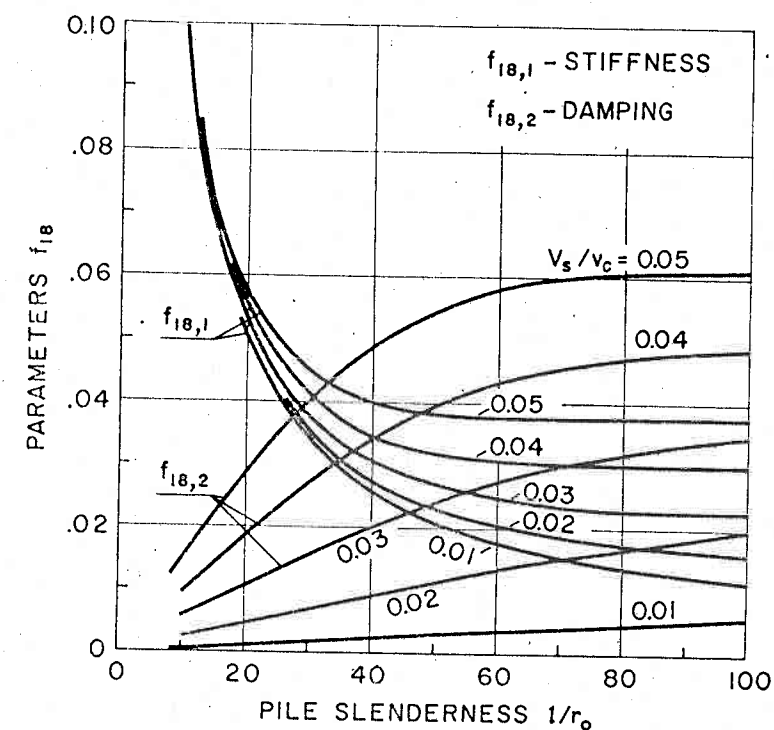
The side reactions result in additional stiffness and damping constants to be added to those derived from piles and given by Eqs. [61] and [62]. The additional stiffness and damping constants of piled footings due to embedment

Response of Pile Foundations

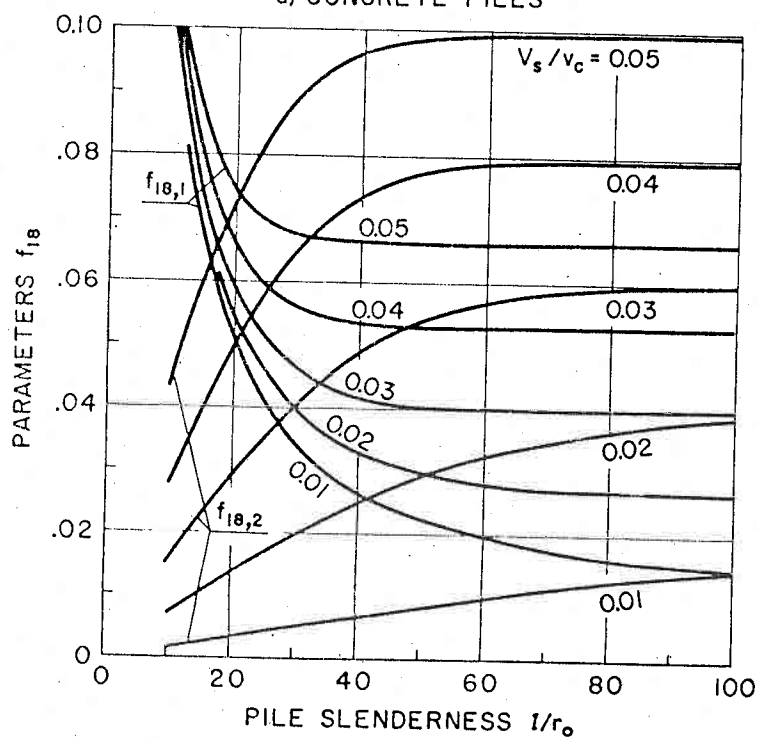
With the stiffness and damping constants defined by Eqs. [61] and [62], the response of footings to dynamic loads can be readily predicted from formulae valid for shallow foundations.

The vertical response to sinusoidal loads can be obtained by means of Eqs. [15]–[18] in Novak and Beredugo 1972.

The response of footings to horizontal excitation and to moments in a vertical plane is always coupled and is characterized by two components, *i.e.* horizontal translation, and



a) CONCRETE PILES



b) WOODEN PILES

FIG. 9. Stiffness and damping parameters of vertical response of (a) reinforced-concrete piles ($\rho/\rho_p = 0.7$), and (b) wooden piles ($\rho/\rho_p = 2.0$).

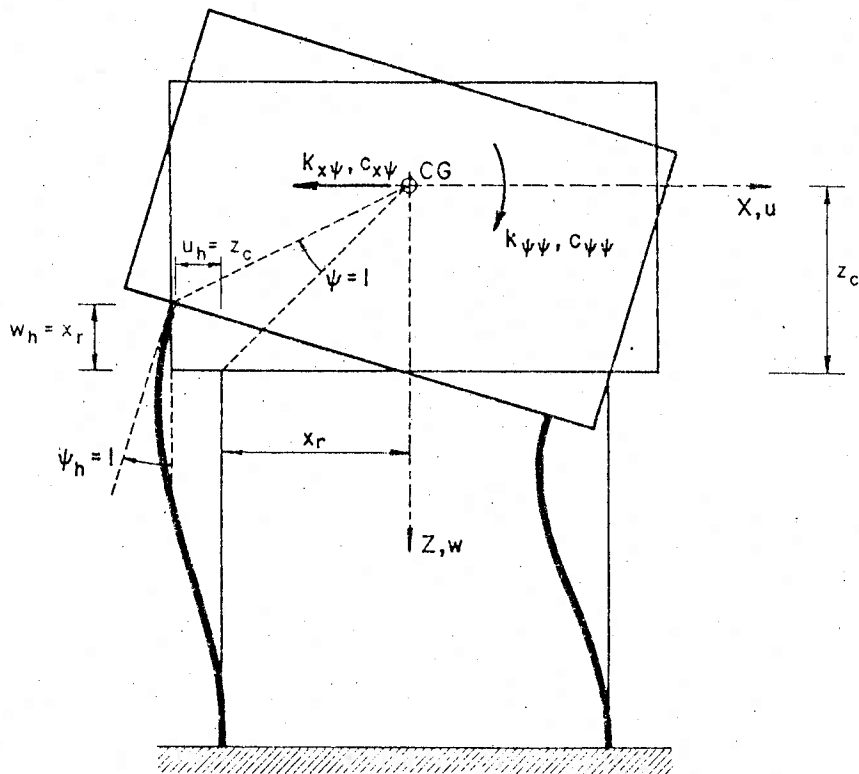


FIG. 10. Pile displacements for determination of footing stiffness and damping constants related to rotation ψ

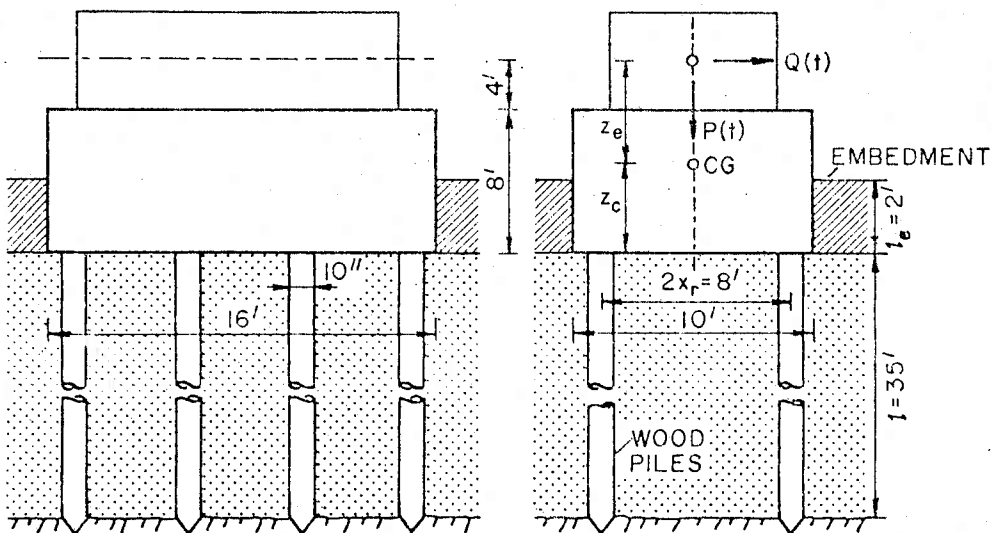


FIG. 11. Dimensions of pile foundation.

rotation in the vertical plane (rocking). The amplitudes of the two components u_0 and ψ_0 follow from Eq. [17] in Beredugo and Novak 1972. With variable frequency of excitation, complete response curves can be obtained.

An alternative approach is to solve the coupled response by means of modal analysis. This approach is outlined in Appendix II where all the formulae needed are given together with the formulae for the natural frequencies and the modal damping pertinent to the two vibration modes of the coupled motion.

Example

The above theory is applied to predict the dynamic response of the machine foundation shown in Fig. 11. The footing is supported by end bearing piles. For comparison, the response is also predicted assuming that the footing rests directly on soil. The effect of a possible embedment is also examined. The following input data are assumed.

The Machine

Total weight = 20 000 lb

Exciting forces due to rotor unbalances act in vertical as well as horizontal directions and are

$$P(t) = m_e e \omega^2 \cos \omega t, \quad Q(t) = m_e e \omega^2 \sin \omega t,$$

where m_e = the mass of the rotor, e = rotor eccentricity, and ω = frequency of rotation. (The true values of $m_e e$ are not chosen as the results will be given in a dimensionless form.) The height of the horizontal excitation = 12 ft which is also the height of the machine centroid.

The Footing

Reinforced concrete, density = 150 lb/ft³, dimensions as shown in Fig. 11.

Embedment depth l_e = 2 ft

The Soil⁴

Bulk density = 100 lb/ft³ ($\rho = 3.11$ slugs/ft³)
Shear wave velocity $V_s = 220$ ft/s ($V_s = \sqrt{G/\rho}$)
Poisson's ratio $\nu = 0.25$

The Backfill

Mass density $\rho_s = 0.75 \rho$
Shear modulus $G_s = 0.5G$

⁴Dynamic properties of soil can be established experimentally or estimated by means of published data (see e.g. Richart *et al.* 1970, Vibrations of soil and foundations, Prentice-Hall Inc., Eaglewood Cliffs, N.J.).

The Piles:⁵

8 soft wood piles

Density = 48 lb/ft³ ($\rho_p = 1.49$ slugs/ft³)

Pile length $l = 35$ ft

Effective radius $r_0 = 5$ in. ($A = 78.54$ in.², $I = 490.9$ in.⁴)

Young's modulus $E_p = 1.2 \times 10^6$ p.s.i. (1.728×10^8 lb/ft²)

Hence, longitudinal wave velocity $v_c = \sqrt{E_p/\rho_p} = 10\,769$ ft/s

Pile eccentricity $x_r = 4$ ft.

With the weights of the footing and the machine, the height of the centroid of the system $z_c = 4.75$ ft, total mass $m = 6583.9$ slugs and the total mass moment of inertia with respect to the centroid $I_\psi = 117\,490.8$ slug ft².

The wave velocity ratio $V_s/v_c = 0.02$. The slenderness ratio $l/r_0 = 84$ is much larger than 25. Therefore all the pile parameters f can be read from Table 1 for the given Poisson's ratio, material ($\rho/\rho_p \approx 2$) and the wave velocity ratio, with the exception of parameters f_{1s} that are obtained from Fig. 9b as $f_{1s,1} = 0.0266$ and $f_{1s,2} = 0.037$.

The constants of one pile are calculated from Eqs. [45] through [60] and with them, the stiffness and damping constants follow from Eqs. [61] and [62].

Then, the response curves are calculated from the formulae given in the references and referred to above. The displacements obtained are those of the centroid.

The response curves of the pile foundation are shown in a dimensionless form in Figs. 12–14 as case A. The crosses (+) indicate approximate resonant amplitudes established by means of simplified modal analysis (Eq. [87], Appendix II). The natural frequencies (Eq. [75]) and modal damping ratios (Eq. [81]) are given in Table 2. Subscript zero denotes the vertical response, subscripts 1 and 2 denote the first and second modes of the coupled response involving horizontal translation and rocking.

Also shown are results calculated for piles and embedment (case B), direct foundation on the soil surface (case C) and for an embedded footing without piles (case D).

When considering the effect of embedment or of soil, the equivalent radii of a circular footing must be used. These can be established from the

⁵Properties of wood piles can be found in Timber Piles, Canadian Institute of Timber Construction, 1962.

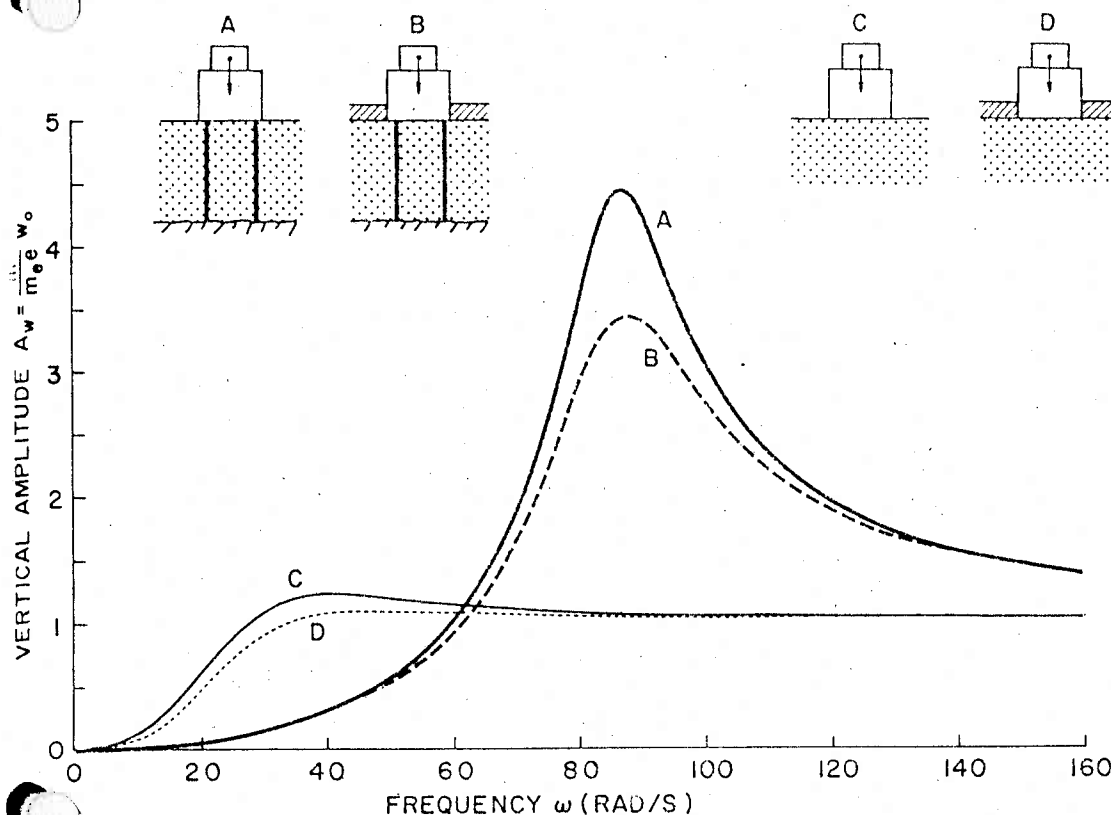


FIG. 12. Vertical response of (A) pile foundation, (B) embedded pile foundation, (C) shallow foundation, and (D) embedded shallow foundation. ($B_x = m/\rho R_x^3 = 5.81$).

equality of the base areas for constants relating to translations (*i.e.* $R_x = 7.14$ ft). For constants relating to rocking, the equivalent radius follows from the equality of the moment of inertia of the base area (*i.e.* $R_y = 6.42$ ft).

Several observations can be made from Figs. 12-14 and from Table 2.

The vibration pattern of pile foundations can considerably differ from that of shallow foundations. The difference is particularly marked in the natural frequencies, resonant amplitudes, and the rocking component of the second mode.

The foundation on piles is more rigid and less damped than that on soil. The resonant amplitudes of the pile foundation can be higher than those of the foundation resting on soil; however, there are frequency regions where the shallow foundation can yield higher amplitudes. The effect of embedment can be very beneficial. Though the piles usually provide the required bearing capacity and reduce permanent settlements, they cannot exclude vibrations.

Effect of Static Axial Load

There is one more aspect which should be considered.

With heavy pile loading and very soft soils, the pile stiffness and damping related to horizontal excitation can be affected by the static load N_{st} the pile carries. This effect brings another parameter into the problem and can be examined as follows:

With soil reaction given by Eq. [1] and the static compressive force $N_{st} > 0$, the differential equation of the pile lateral motion $u(z, t)$ is

$$[63] \quad \mu \frac{\partial^2 u(z, t)}{\partial t^2} + c \frac{\partial u(z, t)}{\partial t} + G(S_{u1} + iS_{u2})u(z, t) + N_{st} \frac{\partial^2 u(z, t)}{\partial z^2} + E_p I \frac{\partial^4 u(z, t)}{\partial z^4} = 0$$

in which μ = mass of the pile per unit length,

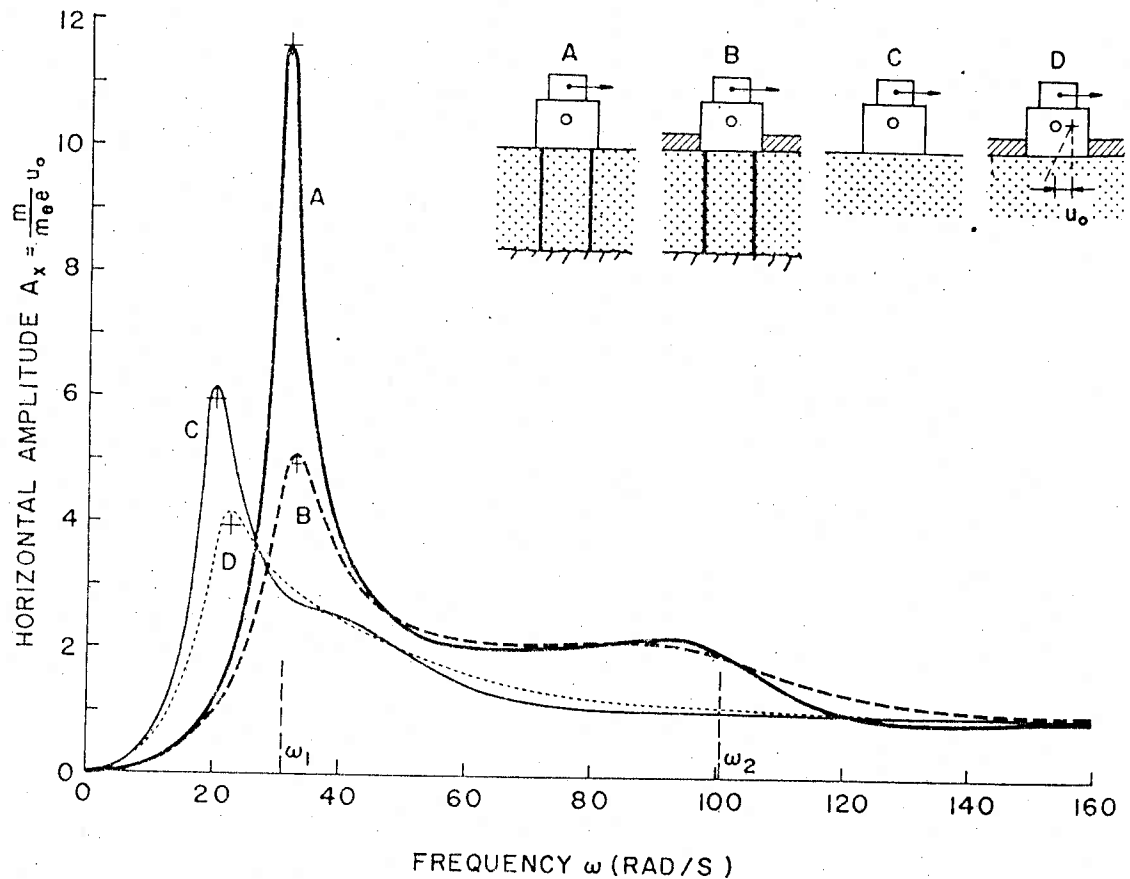


FIG. 13. Horizontal component of coupled footing response to horizontal load. (A) pile foundation, (B) embedded pile foundation, (C) shallow foundation, and (D) embedded shallow foundation, ($B_x = m/\rho R_x^3 = 5.81$, $B_\psi = I_\psi/\rho R_\psi^5 = 3.46$; (+) = modal analysis).

c = coefficient of pile internal damping, $E_p I$ = bending stiffness of the pile and N_{st} = static axial force (load of the pile).

Assume a harmonic motion (induced through the boundary conditions)

$$[64] \quad u(z, t) = u(z) e^{i\omega t}$$

in which complex amplitude

$$[65] \quad u(z) = u_1(z) + i u_2(z)$$

Substitution of Eq. [65] into Eq. [63] yields an

ordinary differential equation

$$[66] \quad E_p I \frac{d^4 u(z)}{dz^4} + N_{st} \frac{d^2 u(z)}{dz^2} + u(z) [GS_{u1} - \mu \omega^2 + i(c\omega + GS_{u2})] = 0$$

The complete integral of this equation is

$$[67] \quad u(z) = C_1 \cosh \lambda \frac{z}{l} + C_2 \sinh \lambda \frac{z}{l} + C_3 \cos \bar{\lambda} \frac{z}{l} + C_4 \sin \bar{\lambda} \frac{z}{l}$$

where

$$[68] \quad \lambda, \bar{\lambda} = \frac{\pi}{\sqrt{2}} \left\{ \mp \frac{N_{st}}{N_E} + \sqrt{\left(\frac{N_{st}}{N_E} \right)^2 - \frac{4E_p I}{N_E^2} [GS_{u1} - \mu \omega^2 + i(c\omega + GS_{u2})]} \right\}^{1/2}$$

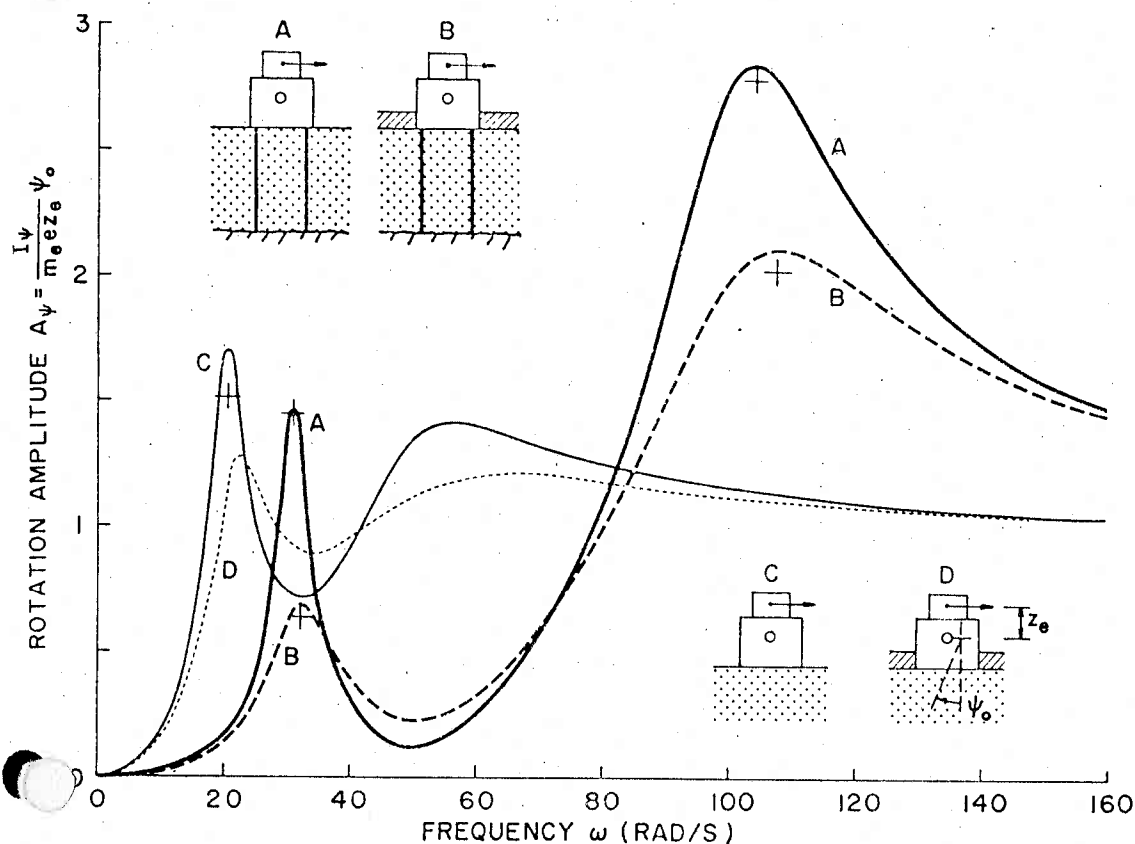


FIG. 14. Rocking component of coupled footing response to horizontal load. (A) pile foundation, (B) embedded pile foundation, (C) shallow foundation, and (D) embedded shallow foundation, ($B_x = 5.81$, $B_\psi = 3.46$, (+) = modal analysis).

and

[69]

$$N_E = \frac{\pi^2 E_p I}{l^2}$$

Note

$$\left\{ \begin{aligned} L &= \frac{l^4 G}{E_p I}, & \lambda_0 &= l \sqrt[4]{\frac{\mu \omega^2}{E_p I}} \\ a &= \frac{\pi^4}{4} \left(\frac{N_{st}}{N_E} \right)^2 + \lambda_0^4 - L S_{u1} \\ b &= -L \left(c \omega \frac{1}{G} + S_{u2} \right) \\ r &= \sqrt{a^2 + b^2}, & \tan \phi &= \frac{b}{a} \\ \bar{a} &= \sqrt{r} \cos \frac{\phi}{2} \mp \frac{N_{st} \pi^2}{N_E} \end{aligned} \right. \quad [70]$$

in the last equation, as well as in Eq. [68], the

minus sign applies for λ and the plus sign belongs to $\bar{\lambda}$. If further

$$[71] \quad b = \sqrt{r} \sin \frac{\phi}{2}, \quad \bar{r} = \sqrt{\bar{a}^2 + \bar{b}^2}, \quad \tan \phi = \frac{\bar{b}}{\bar{a}}$$

then more conveniently

$$[72] \quad \lambda, \bar{\lambda} = \lambda_1 + i \lambda_2$$

in which

$$[73] \quad \lambda_1 = \sqrt{\bar{r}} \cos \frac{\phi}{2}, \quad \lambda_2 = \sqrt{\bar{r}} \sin \frac{\phi}{2}$$

The application of the boundary conditions to the calculation of the integration constants C and pile end reactions is almost the same as in the previous case. The differences are only due to the two parameters λ and $\bar{\lambda}$ appearing in the solution in place of a single one. Therefore,

TABLE 2. Natural frequencies and damping ratios of footing with various types of foundation

Case	Type of foundation	Natural frequency (rad/s)*			Damping percentage*		
		ω_0	ω_1	ω_2	D_0	D_1	D_2
A	Piles	85.5	30.9	100.3	11.2	5.9	15.0
B	Piles and embedment	85.9	31.8	101.5	14.7	14.0	21.0
C	Soil	29.1	19.8	48.7	45.4	13.3	30.5
D	Soil and embedment	30.2	21.0	51.1	54.0	20.3	43.1

*Subscript zero denotes vertical vibration, subscripts 1 and 2 denote the first and second modes of the coupled response.

the pile end forces and moments are again described by Eqs. [19], [20], [22], and [23], in which the functions of argument λ are replaced by somewhat modified functions of two arguments λ and $\bar{\lambda}$. These modified functions do not differ from those for a bare beam (Kolousek 1973) because the effect of soil is confined to the two arguments λ and $\bar{\lambda}$. For the pile having the lower end pinned and the upper end fixed, the following functions apply:

$$\begin{aligned}
 [74] \quad \left\{ \begin{aligned}
 F_7(\lambda, \bar{\lambda}) &= \frac{1}{\phi_1} (\lambda^2 + \bar{\lambda}^2) \sinh \lambda \sin \bar{\lambda} = \\
 &\quad F_7(\lambda, \bar{\lambda})_1 + iF_7(\lambda, \bar{\lambda})_2 \\
 F_8(\lambda, \bar{\lambda}) &= \frac{1}{\phi_1} \lambda \bar{\lambda} (\lambda \sinh \lambda + \bar{\lambda} \sin \bar{\lambda}) = \\
 &\quad F_8(\lambda, \bar{\lambda})_1 + iF_8(\lambda, \bar{\lambda})_2 \\
 F_9(\lambda, \bar{\lambda}) &= \frac{-1}{\phi_1} \lambda \bar{\lambda} (\bar{\lambda} \cosh \lambda \sin \bar{\lambda} \\
 &\quad + \lambda \sinh \lambda \cos \bar{\lambda}) = F_9(\lambda, \bar{\lambda})_1 + iF_9(\lambda, \bar{\lambda})_2 \\
 F_{10}(\lambda, \bar{\lambda}) &= \frac{-1}{\phi_1} \lambda \bar{\lambda} (\lambda^2 \cosh \lambda \\
 &\quad + \bar{\lambda}^2 \cos \bar{\lambda}) = F_{10}(\lambda, \bar{\lambda})_1 + iF_{10}(\lambda, \bar{\lambda})_2 \\
 F_{11}(\lambda, \bar{\lambda}) &= \frac{1}{\phi_1} \lambda \bar{\lambda} (\lambda^2 + \bar{\lambda}^2) \cosh \lambda \cos \bar{\lambda} = \\
 &\quad F_{11}(\lambda, \bar{\lambda})_1 + iF_{11}(\lambda, \bar{\lambda})_2
 \end{aligned} \right.
 \end{aligned}$$

in which

$$\phi_1 = \lambda \cosh \lambda \sin \bar{\lambda} - \bar{\lambda} \sinh \lambda \cos \bar{\lambda}$$

Similar functions can be found for the other boundary conditions.

Stiffness and damping coefficients of piles are obtained by the substitution of the real and imaginary parts of functions $F(\lambda, \bar{\lambda})$ in

Eqs. [49]–[60] in place of functions $F(\lambda)$ having the same subscripts.

An example of the static load effect is shown in Fig. 15. It can be seen that the general effect of the static load is to reduce the stiffness and damping parameters with the exception of $f_{7,2}$ that increases and $f_{9,1}$ and $f_{11,2}$ that remain almost independent of N_{st} .

The magnitude of the variations due to N_{st} depends primarily on soil stiffness (wave velocity ratio) and on the slenderness ratio. With increasing soil stiffness, the effect of the static load diminishes; it is negligible for wave velocity ratio = 0.03 and with all the other parameters remaining the same as in Fig. 15.

The effect of a certain N_{st} should also diminish with decreasing slenderness. For slenderness ratios greater than 30, the parameter variations with a certain N_{st} should be about the same as for $l/r_0 = 30$ because any further increase in pile length changes the stiffness and damping parameters only very slightly. In most practical cases the effect of N_{st} will be negligible. (N_E is very large in the shown case.)

Summary and Conclusions

The dynamic stiffness and geometric damping of piles depend on soil–pile interaction and are governed by the following dimensionless parameters: specific mass of the soil over specific mass of the pile (mass ratio), shear wave velocity in the soil over longitudinal wave velocity in the pile (wave velocity ratio), length of the pile (thickness of the soil layer) over pile radius (slenderness ratio), pile static load over Euler's buckling load (load ratio), and the dimensionless frequency.

The most important parameters are the wave velocity ratio and the slenderness ratio.

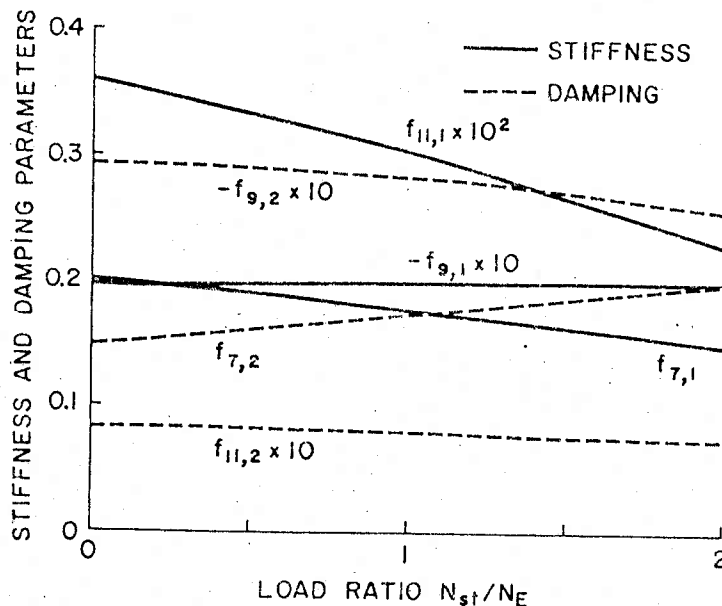


FIG. 15. Variations of stiffness and damping parameters with static load, ($l/r_0 = 30$, $V_s/v_c = 0.01$, $\rho/\rho_p = 0.7$, $\nu = 0.4$, $a_0 = 0.3$).

Both pile stiffness and damping increase with increasing wave velocity ratio and with increasing static load. Dynamic stiffness and damping with horizontal excitation are very sensitive to the pile length for a slenderness l/r_0 smaller than about 25 and practically independent of the pile length for l/r_0 greater than this limit. Above the same limit, the influence of the end condition at the pile tip vanishes; this means that there is no appreciable difference between a pinned tip and a fixed tip and that further increase in pile length does not affect the dynamic stiffness and the damping. The limit to the effect of the pile length is somewhat dependent on the stiffness of the soil. The relatively low limit to the effect of the pile length makes it possible to present numerical values of stiffness and damping parameters valid for most practical situations.

In the vertical direction, the effect of pile length does not diminish within the practical range of slendernesses because the stiffness of the pile alone compares more favourably with that of soil than is the case with horizontal excitation. However, the stiffness and damping parameters for the vertical direction are given in graphical form to cover most practical applications.

The effect of the static load can be significant only with extremely poor soils. The static

load reduces most stiffness and damping parameters, but increases damping due to rotation.

For all possible displacements the pile stiffness and geometric damping can be readily established; hence, the response of footings or structures supported by piles can be obtained by the same procedure as is applied with shallow foundations.

Pile foundations can have higher natural frequencies, smaller damping and larger resonant amplitudes than footings founded directly on soil.

The piles can eliminate or reduce permanent settlements; however, they cannot eliminate vibrations. Dynamic analysis is just as important with pile foundations as it is with shallow foundations.

The approach presented is approximate and yields somewhat lower stiffnesses and damping than the more rigorous elastic model. This may be considered on the safe side as the bond between the pile and the soil is not perfect as is assumed in the dynamic elastic solution.

The approximate analytical solution may help to specify the dimensionless parameters and to indicate appropriate ranges for more rigorous approaches where much higher computing costs will be involved.

Experiments are needed to verify the theory and to estimate the effect of pile grouping and other components of damping acting jointly with the geometric damping considered in this paper.

Acknowledgments

This study was supported by a research grant from the National Research Council of Canada. The assistance of T. Nogami is gratefully acknowledged.

- BARANOV, V. A. 1967. On the calculation of excited vibrations of an embedded foundation. (*in Russian*). Voprosy Dynamiki Prochnosti, No. 14, Polytech. Inst. Riga, pp. 195-209.
- BARKAN, D. D. 1962. Dynamics of bases and foundations. McGraw-Hill Book Company, New York, N.Y.
- BEREDUGO, Y. O., and NOVAK, M. 1972. Coupled horizontal and rocking vibration of embedded footings. Can. Geotech. J. 9(4), pp. 477-497.
- KOLOUSFK, V. 1973. Dynamics in engineering structures. Halsted Press, a Division of John Wiley and Sons, New York, N.Y.
- NOVAK, M., and BEREDUGO, Y. O. 1972. Vertical vibration of embedded footings. J. Soil Mech. Found. Div., A.S.C.E., 12, pp. 1291-1310.
- NOVAK, M., and SACHS, K. 1973. Torsional and coupled vibrations of embedded footings. Int. J. Earthquake Eng. Struct. Dyn., J. Wiley and Sons, 2(1), pp. 11-33.
- NOVAK, M. 1974. Effect of soil on structural response to wind and earthquake. Int. J. Earthquake Eng. Struct. Dyn., J. Wiley and Sons, 3(1), pp. 79-96.
- PENZIN, J. 1970. Soil-pile foundation interaction. In Earthquake engineering. Edited by Wiegell, R. L. Prentice-Hall, Inc., Eaglewood Cliffs, N.J., pp. 349-381.
- POULOS, H. G. 1971. Behavior of laterally loaded piles: II. Piles groups. J. Soil Mech. Found. Div., A.S.C.E., 97(SM5), pp. 733-751.
- POULOS, H. G. 1973. Behavior of laterally loaded piles: III. Socketed piles. J. Soil Mech. Found. Div., A.S.C.E., 98(SM4), pp. 341-360.
- RAUSCH, E. 1959. Maschinenfundamente. VDI-Verlag GmbH., Düsseldorf, Ger. (*in German*).
- TAJIMI, H. 1966. Earthquake response of foundation structures. Report of the Faculty of Science and Engineering, Nihon University, Tokyo City, Jap., pp. 1.1-3.5 (*in Japanese*).
- D = damping ratio of footing
- c = coefficient of pile internal viscous damping
- $c_{i,j}$ = damping constant of footing
- $c_{i,j}^1$ = damping constant of one pile
- E_p = Young's modulus of pile
- F_i = frequency functions
- e = eccentricity of unbalanced mass
- $f_{j,1}$ = stiffness parameters of pile
- $f_{j,2}$ = damping parameters of pile
- G = shear modulus of soil
- I = moment of inertia of pile cross section
- I_ψ = mass moment of inertia of footing
- i = $\sqrt{-1}$ = imaginary unit
- K = dimensionless parameter
- $k_{i,j}$ = stiffness constant of footing
- $k_{i,j}^1$ = stiffness constant of one pile
- L = dimensionless parameter
- l = length of pile, thickness of soil layer
- l_e = foundation embedment
- M = bending moment of pile
- m = mass of footing
- m_e = unbalanced mass
- N = axial (normal) force in pile
- N_E = Euler's buckling load
- N_{st} = static load of the pile
- R_i = pile reaction in direction i
- $R_{x,\psi}$ = equivalent footing radius for directions x or ψ respectively
- r_0 = radius of pile, equivalent radius of pile for noncircular piles
- S_{u1} = real part of layer reaction in horizontal direction
- S_{u2} = imaginary part of layer reaction in horizontal direction
- S_{w1} = real part of layer reaction in vertical direction
- S_{w2} = imaginary part of layer reaction in vertical direction
- T = shear force in pile
- t = time
- u = horizontal translation of pile
- u_h = horizontal translation of pile head
- u_g = horizontal translation of pile tip
- u_0 = amplitude of horizontal vibration of footing
- $u_{1,2}$ = real and imaginary parts of u
- V_s = $\sqrt{G/\rho}$ = shear wave velocity of soil
- v_c = $\sqrt{E_p/\rho_p}$ = longitudinal wave velocity in pile
- w = vertical displacement of pile
- w_h = vertical displacement of pile head
- w_g = vertical displacement of pile tip

Appendix I - Notation

The following symbols are used in this paper:

- A = area of pile cross section
- A_i = dimensionless amplitude of footing in direction i
- a = parameter
- a_0 = $r_0 \omega \sqrt{\rho/G}$ = dimensionless frequency
- b = parameter
- C_i = integration constant

- = amplitude of vertical vibration of footing
- = horizontal distance of pile from reference point
- = vertical coordinate
- = height of centroid above base
- = height of excitation above centroid
- = frequency parameter for vertical response
- = frequency parameter of pile alone
- = real and imaginary parts of Λ
- = frequency parameter for horizontal excitation
- = real and imaginary parts of λ
- = mass density of soil
- = mass density of pile
- = rotation in vertical plane
- = rotation of pile head in vertical plane
- = amplitude of footing rocking
- = circular excitation frequency
- = natural frequency of vertical vibration
- = natural frequencies of coupled motion

Assume excitation by harmonic horizontal force $Q(t)$ and moment $M_e(t)$ (Fig. 11)

$$[77] \quad Q(t) = Q_0 (\sin \omega t)$$

$$[78] \quad M(t) = M_0 \sin \omega t = (Q_0 z_e + M_e) \sin \omega t$$

The generalized force amplitudes, producing response in one mode each, (Fig. 16), are

$$[79] \quad p_j = Q_0 u_j + M_0 \psi_j$$

and the generalized masses

$$[80] \quad M_j = m u_j^2 + I_\psi \psi_j^2$$

in which subscript $j = 1, 2$ denotes the mode and the corresponding frequency. The modal coordinates u_j and ψ_j can be chosen in an arbitrary scale; e.g. $\psi_j = 1$ and thus from Eq. [76], $u_j = a_j$.

The two modal damping ratios pertinent to the vibration modes are from Eq. 21 in Novak 1974

$$[81] \quad D_j = \frac{1}{2\omega_j M_j} (c_{xx} u_j^2 + c_{\psi\psi} \psi_j^2 + 2c_{x\psi} u_j \psi_j)$$

in which damping constants c are given by Eqs. [51]–[60]. Then the footing translation and rocking are

$$[82] \quad u(t) = \sum_{j=1}^2 q_j u_j \sin(\omega t + \phi_j)$$

$$[83] \quad \psi(t) = \sum_{j=1}^2 q_j \psi_j \sin(\omega t + \phi_j)$$

in which the amplitudes of the generalized coordinates

$$[84] \quad q_j = \frac{p_j}{M_j \sqrt{(\omega_j^2 - \omega^2)^2 + 4(D_j \omega_j \omega)^2}}$$

and the phase shifts

$$[85] \quad \phi_j = -a \tan \frac{2D_j \omega_j \omega}{\omega_j^2 - \omega^2}$$

With respect to the phase difference between ϕ_1 and ϕ_2 the true amplitudes of translation u_0 and rocking ψ_0 are the vector sum of the two modal components, i.e.

$$u_0 = \sqrt{(q_1 u_1 \sin \phi_1 + q_2 u_2 \sin \phi_2)^2 + (q_1 u_1 \cos \phi_1 + q_2 u_2 \cos \phi_2)^2}$$

analogous equation for ψ_0 .

Appendix II – Solution of Coupled Motion by Means of Modal Analysis

Practical predictions of amplitudes of the coupled motion involving sliding u and rocking ψ by modal analysis is very suitable. The method described in general by Novak 1974. The formulae applicable to footings are summarized below.

With stiffnesses given by Eqs. [49]–[58], the two natural frequencies follow from the formula

$$\omega_{1,2}^2 = \frac{1}{2} \left(\frac{k_{xx}}{m} + \frac{k_{\psi\psi}}{I_\psi} \right) \mp \sqrt{\frac{1}{4} \left(\frac{k_{xx}}{m} - \frac{k_{\psi\psi}}{I_\psi} \right)^2 + \frac{k_{x\psi}^2}{m I_\psi}}$$

the two natural modes (ratios of displacements) are

$$a_j = \frac{u_j}{\psi_j} = \frac{-k_{x\psi}}{k_{xx} - m\omega_j^2} = \frac{k_{\psi\psi} - I_\psi \omega_j^2}{-k_{x\psi}} \quad \text{with } j = 1, 2$$

For correct values of ω_1 and ω_2 and constant parameters, both equations must give the same value which is a quick check.)

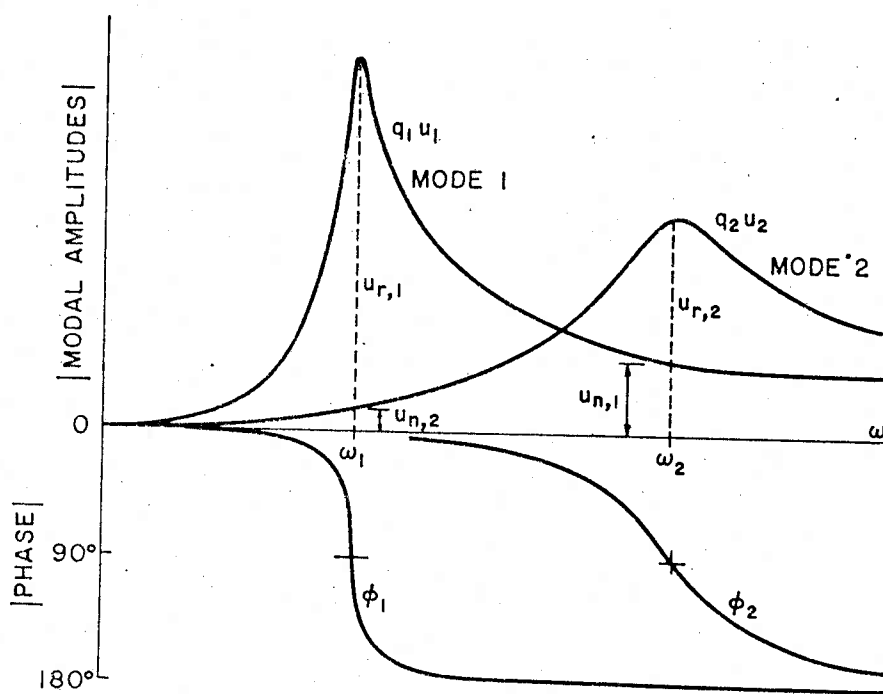


FIG. 16. Modal superposition of footing response, (excitation proportional to ω^2).

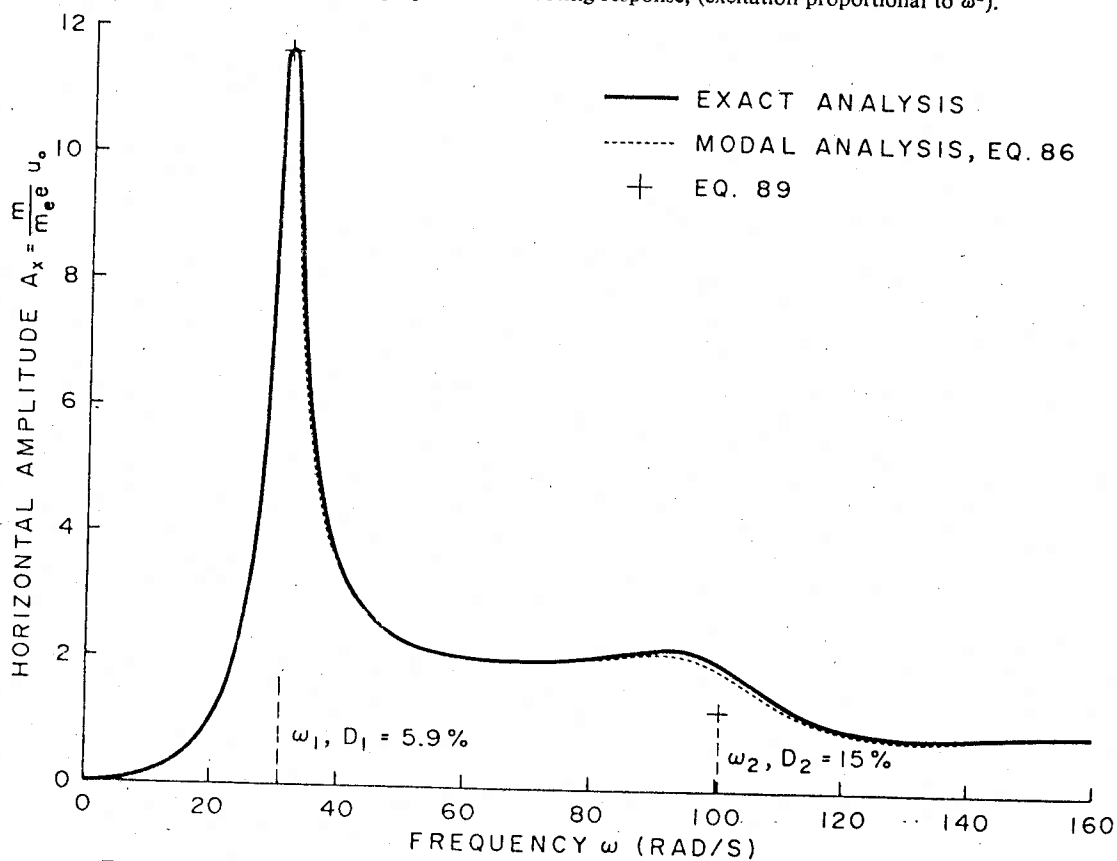


FIG. 17. Sliding component of coupled response computed directly (exactly) and by means of modal analysis, (for foundation shown in Fig. 11).

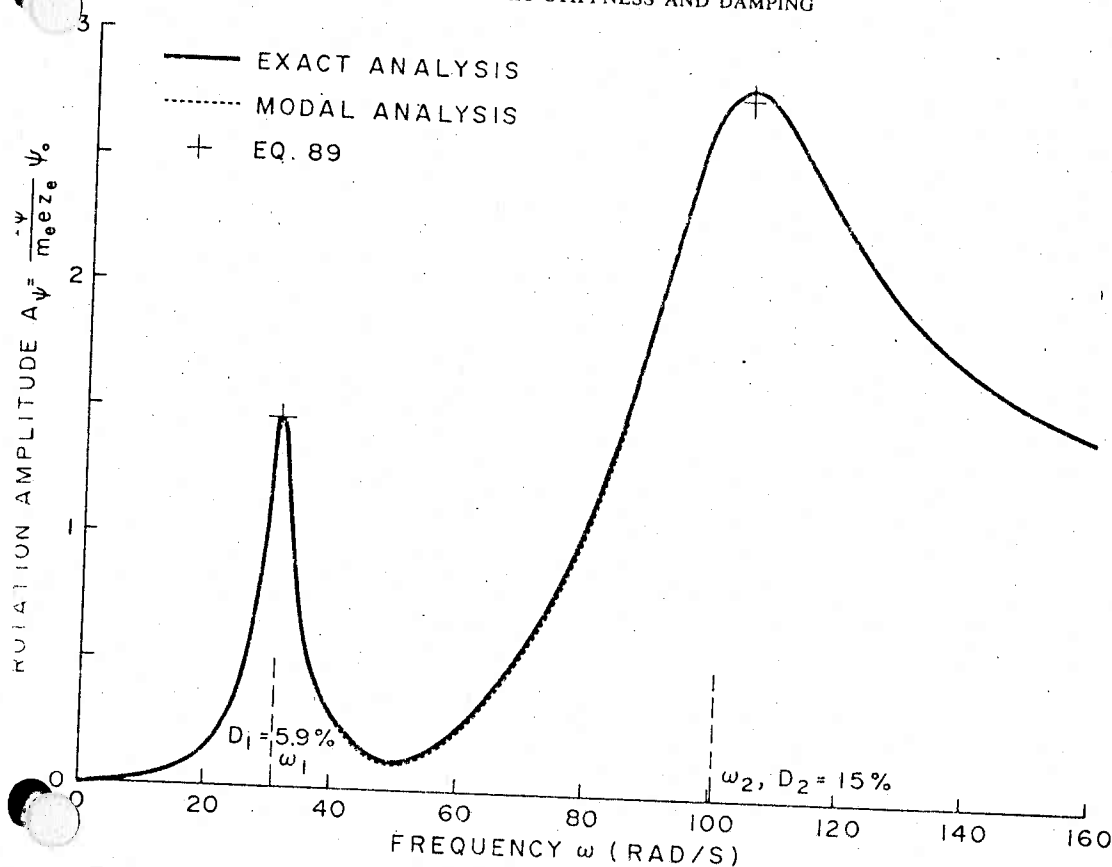


Fig. 18. Rocking component of coupled response computed directly (exactly) and by means of modal analysis, (for foundation shown in Fig. 11).

Equation [86] gives results usually very close to those obtained by direct calculation from Figs. 17 in Beredugo and Novak 1972 (Figs. 17 and 18).

A significant simplification can be achieved when calculating the maximum amplitude in the first or second resonant peaks of the coupled motion (Figs. 17 and 18). When the damping of the resonating mode is not too large and the response curve shows a peak, the contribution of the nonresonant modal component to the resonant amplitude can be neglected in most cases because it is small and the phase difference between the two components is close to 90° (Fig. 16). Then the resonant amplitudes of the coupled motion at resonance j ($j = 1$ or 2) are approximately

$$u_{r,j} = \frac{p_j u_j}{2D_j M_j \omega_j^2}$$

$$\psi_{r,j} = \frac{p_j \psi_j}{2D_j M_j \omega_j^2}$$

The resonant amplitudes calculated from the very simple Eqs. [87] are shown as crosses (+) in Figs. 13 and 14. The agreement between the accurate and approximate values is quite good. The agreement can be further improved by the vector addition of the nonresonating mode obtainable from Eq. [84]. With the omission of damping, possible with respect to large differences between ω_1 and ω_2 , the amplitudes of the nonresonating mode k at frequency ω_j are

$$[88] \quad u_{n,k} = \frac{p_k u_k}{M_k(\omega_2^2 - \omega_1^2)}$$

$$\psi_{n,k} = \frac{p_k \psi_k}{M_k(\omega_2^2 - \omega_1^2)}$$

Because the phase shift between the resonating and nonresonating modes is close to 90°, the resonant amplitudes are approximately

$$[89] \quad \begin{aligned} \hat{u}_j &= \sqrt{\frac{u_{r,j}^2 + u_{n,k}^2}{1 - D_j^2}} \\ \hat{\psi}_j &= \sqrt{\frac{\psi_{r,j}^2 + \psi_{n,k}^2}{1 - D_j^2}} \end{aligned}$$

in which $k \neq j$.

The inclusion of the damping in the denominator yields the approximate value of the maximum resonant amplitude instead of the somewhat smaller amplitude at frequency ω_j . (The maximum amplitude does not appear exactly at ω_j .)

Equations [89] yield an even better estimate of the resonant amplitudes than Eqs. [87] alone. The amplitudes calculated from Eqs. [89] are shown in Figs. 17 and 18 where the complete response curves, obtained directly and by means of modal analysis, are also plotted. The agreement between the two approaches is very good.

The same modal approach can be used with shallow foundations. The only difference is in the stiffness and damping constants which can be obtained from Beredugo and Novak 1972 or Novak 1974.